7-28-2022

Distinct Temporal and Mechanistic Contributions of the Hippocampus, Striatum, and Medial Prefrontal Cortex Facilitate Memory-Guided Decision-Making

Amanda G. Renfro
Florida International University, neuronmage@gmail.com

FLORIDA INTERNATIONAL UNIVERSITY

Miami, Florida

DISTINCT TEMPORAL AND MECHANISTIC CONTRIBUTIONS OF THE HIPPOCAMPUS, STRIATUM, AND MEDIAL PREFRONTAL CORTEX FACILITATE MEMORY-GUIDED DECISION MAKING

A dissertation submitted in partial fulfillment of

the requirements for the degree of

DOCTOR OF PHILOSOPHY

in

COGNITIVE NEUROSCIENCE

by

Amanda G. Renfro

2022

To: Dean Michael R. Heithaus
College of Arts, Sciences, and Education

This dissertation, written by Amanda G. Renfro, entitled Distinct Temporal and Mechanistic Contributions of the Hippocampus, Striatum, and Medial Prefrontal Cortex Facilitate Memory-Guided Decision Making, having been approved in respect to style and intellectual content, is referred to you for judgment.

We have read this dissertation and recommend that it be approved.

_____
Timothy Allen

_____
Fabian Soto

_____
Kim Tieu

_____
Aaron T. Mattfeld, Major Professor

Date of Defense: July 28, 2022

The dissertation of Amanda G. Renfro is approved.

_____
Dean Michael R. Heithaus
College of Arts, Sciences and Education

_____
Andrés G. Gil
Vice President for Research and Economic Development
and Dean of the University Graduate School

Florida International University, 2022

DEDICATION

I dedicate this dissertation to my wonderful parents, Duard and Helen Hamm,

who always encouraged me to pursue my passions.

ACKNOWLEDGMENTS

First and foremost, I must express my admiration and appreciation for my major professor, Dr. Aaron Mattfeld, for his professional guidance, training, sage advice, patience, and friendship. Dr. Mattfeld has provided me a wonderful research environment in which to develop my scientific acumen, programming skills, and understanding of how to navigate academia. Most of all, he is a terrific mentor and friend, who has encouraged and cultivated a greatness in me I could not always see for myself. Secondly, I would like to sincerely thank each of my esteemed dissertation committee members: Dr. Timothy Allen, thank you for serving as my unofficial co-mentor and friend, as well as granting me the opportunity to experience all the joys of animal work; Dr. Fabian Soto, thank you for your kind and patient guidance and expertise in computational modeling, not to mention your friendship and online game-nights with your team; and Dr. Kim Tieu, thank you for your gentle and kind words of encouragement which helped raise my spirits in times of stress and self-doubt. Thirdly, I would like to thank my lab family, both those still here and those who have moved on, for all their contributions to my scientific endeavors. Finally, I would like to express my gratitude to my amazing friends who, in many ways, helped me become the scientist I am today: Jason Hays, for teaching me how to program like a boss; Maanasa Jayachandran, for the late nights teaching me to build drivable tetrode head-stages; and Adam Kimbler, for his gentle friendship and support.

Getting to this point in my life and career was certainly a team effort, and I would like to thank everyone who contributed to helping me achieve my dreams.

ABSTRACT OF THE DISSERTATION

DISTINCT TEMPORAL AND MECHANISTIC CONTRIBUTIONS OF THE HIPPOCAMPUS, STRIATUM, AND MEDIAL PREFRONTAL CORTEX FACILITATE MEMORY-GUIDED DECISION MAKING

by

Amanda G. Renfro

Florida International University, 2022

Miami, Florida

Professor Aaron T. Mattfeld, Major Professor

In this dissertation, I investigate how the hippocampus, medial prefrontal cortex and striatum facilitate memory-guided decision making. While a great deal of human and animal research has been dedicated to solving this puzzle, much of this work has focused on “retrospective” mechanisms of this process. Although retrieval and deliberation are certainly fundamental elements of successful choice behavior, how these regions prospectively support memory-guided decision making is also worthy of further study. Here, I present: (1) elucidation of two distinct networks which support prospective and concurrent memory-guided behavior, (2) evidence hippocampal support to experience-based learning is a dynamic, evolving process, and (3) demonstration of prospective representational content using machine learning. In my first experiment, participants completed a visuospatial conditional associative task (vCAT1) in which correct conditional response was dependent on the preceding stimulus. Through both uni- and multivariate methods, I demonstrate evidence of two separate networks through

which memory guides decision making behavior: (1) hippocampus (HPC), putamen (PUT), medial prefrontal cortex (mPFC), and other cortical regions which showed increased activation preceding successful conditional choice, and (2) dorsal anterior caudate (DAC), dorsolateral prefrontal cortex (dlPFC), and other cortical regions, which exhibited increased activation during successful choice execution. In order to address how these regions and their collaborative contributions may evolve across learning, I employed two learning analyses to determine how HPC and DAC support early and late learning. I observed decreased activation for DAC as performance improved and selective involvement of the HPC for late, but not early learning. These findings demonstrate dynamic contributions of the HPC as learning develops. In my second experiment, participants completed a more complex visuospatial conditional associative task (vCAT2) to reduce ceiling effects and prevent alternating response set. Here, I collected data for purposes of conducting a multivoxel pattern analysis to investigate neurobiological representations of prospective memory. Classifier accuracy for both FFA and PPA was better than would be expected by chance, but no statistically significant relationship was observed between classifier and subject performance. These findings provide evidence for prospective representational content which supports memory-guided decision making processes.

TABLE OF CONTENTS

CHAPTER PAGE

LIST OF TABLES

TABLE PAGE

LIST OF FIGURES

FIGURE PAGE

ABBREVIATIONS AND ACRONYMS

ACC	Anterior Cingulate Cortex
BL	Perceptual Baseline Trials
BOLD	Blood-Oxygen Level Dependent
DAC	Dorsal Anterior Caudate
dlPFC	Dorsolateral Prefrontal Cortex
fMRI	Functional Magnetic Resonance Imaging
FOV	Field of View
HPC	Hippocampus
IQR	Inter-Quartile Range
LSS	Least Squares Single Method
mPFC	Medial Prefrontal Cortex
OG	Object Group
PCC	Posterior Cingulate Cortex
PUT	Putamen
ROI	Region of Interest
SD	Standard Deviation
SWR	Sharp-Wave Ripples
TE	Echo Time
TFCE	Threshold-Free Cluster Enhancement
TR	Repetition Time

CHAPTER 1: INTRODUCTION

A critical element of decision making is the ability to apply personal experience to present circumstance. More specifically, our memory concerning relationships between discrete events, as well as subsequent outcomes, is necessary to inform behavior and selection of situationally optimal choices. To date, animal and human work have investigated ways in which memory informs and directs our choices (Bornstein et al., 2017; Gluth et al., 2015; Jadhav et al., 2012; Murty et al., 2016; J. P. O'Doherty et al., 2017; Pfeiffer & Foster, 2013; Shohamy & Daw, 2015; Weber et al., 1993; Wimmer & Shohamy, 2012; Zeithamova, Dominick, et al., 2012), but much of this research has focused on "retrospective" mechanisms of memory. Although retrieval, and integration of past associations with current circumstance, certainly offer important insight into neurobiological mechanisms for behavior, the scope of investigation into memory-guided decision making should not be limited to only those dynamics observed at time of choice. Prospective memory, or the neurobiological processes supporting realization of intended future choice, also contributes to successful behavior (Kvavilashvili, 1987). Prospective memory is a multifaceted phenomenon which includes retrieval of content regarding relevant behavior, deliberate maintenance of information in working memory with imminent intent, and concurrent execution (Monti et al., 2020). Thus, prospective memory is theorized to include four unique subprocesses: (1) formation of intention, (2) retention of intention, (3) re-instantiation of intention, and finally (4) execution of intended behavior (Cohen & O'Reilly, 1996; Ellis, 1996; Kliegel et al., 2002).

Two regions implicated in prospective memory processes across both human and animal work are the hippocampus (HPC; Benchenane et al., 2010; Cohen & O'Reilly, 1996; Euston et al., 2012; Jadhav et al., 2012, 2016; Pfeiffer & Foster, 2013; Shin & Jadhav, 2016; Wang & Morris, 2010; Yu & Frank, 2015) and medial prefrontal cortex (mPFC; Benoit et al., 2012; Burgess et al., 2003; de la Vega et al., 2016; Gilbert et al., 2005a; Gilbert, 2011; Haynes et al., 2007; Momennejad & Haynes, 2013, 2012; Okuda et al., 2007; Simons et al., 2006; Soon et al., 2008; Volle et al., 2011). The HPC is understood to acquire and maintain relational representations (Eichenbaum & Cohen, 1988; Squire et al., 2004; Tse et al., 2007), as well as support imaginings of the future (Addis et al., 2007). Similarly, the mPFC, rich in connections to a host of cortical and sub-cortical regions (Preston & Eichenbaum, 2013), is anatomically positioned to support memory formation and retrieval, integrate memories across events (Zeithamova & Preston, 2010), and facilitate decision making (Shin & Jadhav, 2016). A third region worthy of consideration is the striatum. While not directly implicated using most prospective paradigms, the striatum is essential for decision-relevant processes such as response preparation, reward expectation, prediction error, and instrumental learning and memory (Doll et al., 2015; Schultz et al., 2003; Tremblay et al., 1998).

The timing and degree to which contributions of the HPC, mPFC, and striatum prospectively support memory-guided decision making, how such contributions develop across learning, and what sort of representational content can be decoded from patterns of activation during periods of prospective behavior, have not yet been demonstrated. However, previous findings have shown predictive activations

in HPC during statistical learning studies (Bornstein & Daw, 2012; Ferbinteanu & Shapiro, 2003; Schapiro et al., 2012), as well as response preparation and prediction error in the striatum for reward learning tasks (Bornstein & Daw, 2012; Doll et al., 2015).

1.1 PURPOSE

The purpose of my dissertation work was to investigate how the brain supports memory-guided decision making and how such support may evolve across learning. Here, I focused on four primary regions of interest: hippocampus (HPC), medial prefrontal cortex (mPFC), as well as the dorsal anterior caudate (DAC) and putamen (PUT) of the striatum. My objective was not only to elucidate potential mechanisms and timing of these regional contributions, but to understand how these contributions evolve with experience-based learning and to investigate possible representational content maintained prior to decision making by using a complex, multivariate technique known as multivoxel pattern analysis (MVPA). Efforts to better our understanding of these processes may help not only inform the treatment of patients with various types of executive dysfunction, but to guide educational initiatives as well.

1.2 Research questions

1.2.1 Aim 1: Determine contributions of the hippocampus, medial prefrontal cortex, and striatum during prospective and concurrent memory-guided decision making.

In pursuit of Aim 1 (see Chapter 2), participants completed a conditional associative learning task while in a magnetic resonance imaging (MRI) scanner. Here, I sought to determine mechanisms and timing of HPC, mPFC, and striatal contributions to prospective memory-guided decision making. I expected to observe increased prospective activations in HPC, mPFC (defined structurally as the anterior cingulate cortex; or ACC), and dorsal anterior caudate (DAC) preceding correct, compared to incorrect, conditional trials given their association with relational memory, memory integration, and goal-directed action, respectively. I anticipated putamen (PUT) would demonstrate no such distinction in prospective activations. Here, I demonstrated greater activations in HPC, mPFC, and PUT (prospective network) precede successful conditional decision making, while greater activations in DAC and dorsolateral prefrontal cortex (concurrent network) are associated with execution of successful decisions (Hamm & Mattfeld, 2019).

1.2.2 Aim 2: Elucidate how contributions of these cortical and subcortical regions to memory-guided decision making change across learning.

For Aim 2 (see Chapter 3), I expanded on previous analyses to investigate how contributions of HPC, mPFC, and striatum develop across learning. Generally, I predicted (1) increased engagement of HPC, mPFC, and PUT as performance

improved, and (2) decreased DAC activation during this same period. To test these hypotheses, I employed two analytic techniques:

a) *Pattern Dissimilarity Analysis.* First-level analyses were conducted on unsmoothed data, followed by fixed-effect analyses to quantify dissimilarity of activation patterns during periods of early and late learning. Regressors of interest included *fixed trials preceding correct conditional trials* and *fixed trials preceding incorrect conditional trials*. For each run, correlation values were obtained between voxel-wise activation patterns for *fixed trials proceeding correct, versus incorrect, conditional trials* in both HPC and DAC using anatomically defined ROI masks. Dissimilarity value was calculated as 1 – r. First, t-tests (*or Wilcoxon ranked-sign tests*) determined whether statistically significant differences between early or late learning were observed for either HPC or DAC. Second, correlation values between pattern dissimilarity and performance on conditional trials for both early and late learning were calculated. I predicted increased pattern dissimilarity during late, compared to early, learning. Additionally, I expected to observe a positive relationship for pattern dissimilarity and performance across learning for HPC, but not DAC. During periods preceding conditional trial performance, HPC pattern dissimilarity was greater for late, compared to early, learning. In addition, a significant relationship was observed between HPC pattern dissimilarity and learning performance for late, but not early, learning. Similarly, DAC pattern dissimilarity was greater for late, compared to early, learning; however,

significant positive correlations between DAC pattern dissimilarity and learning were observed for both early and late learning.

b) *Binned Learning Curve Analysis*. Three learning bins were created using a flexible algorithm which accounted for differences in participant performance. Conditional trials were numerically organized by probability of correct response (hereafter referred as *PC value*) with minimum and maximum values identified for each participant. Based on participant-specific ranges, the first third of trials (*beginning with lowest PC value*) constituted Learning Bin 1, second third Learning Bin 2, and final third (*ending in highest PC value*) Learning Bin 3. Each model included separate regressors for all bins and regressors of no interest. Anatomical bilateral ROIs were created for HPC and DAC, comparing second-level mean activation for conditional trials during each learning bin. During conditional trial performance, HPC demonstrated greater activation during conditional trials for Bin 3 compared to Bin 1; however, no significant differences were observed when an analysis of variance (ANOVA) considered all three bins. Interestingly, and contrary to my initial predictions, decreased activation was observed for DAC across bins. Simple effect analysis revealed DAC exhibited decreased activation for Bin 3 compared to Bin 1. No significant differences were evident between Bins 3 and 2; although a slight trend of decreased activation for Bins 2 compared to Bin 1 was observed.

1.2.3 **Aim 3: Investigate multivariate neurobiological representations which underlie prospective memory-guided decision making.**

My first two aims investigated contributions of HPC, mPFC, and striatum to prospective and concurrent networks underlying conditional memory-guided

decision-making and how those contributions develop across learning. My third and final aim (see Chapter 5) sought to investigate neurobiological representation of prospective memory using multivoxel pattern analysis (MVPA). MVPA identifies information through patterns in neural response, operationalized in my experiment as voxels (Weaverdyck et al., 2020). Here, I investigated representational content maintained by participants prior to conditional trials by isolating voxel activation patterns in the fusiform face area (FFA) and parahippocampal place area (PPA) during prospective memory-guided behavior. A functional localizer task was used to isolate individual participant activation when presented with faces and scenes, which was then combined with anatomical ROI masks to obtain voxels at the intersection of these two masks. The resulting constrained masks were then applied to vCAT2 first-level copes during fixed trials preceding baseline and conditional trials to provide features required to train a supervised learning algorithm (support vector machine classifier, or SVC). Classifier performance exceeded chance for both FFA and PPA; but no significant relationships between classifier and participant performance was observed.

CHAPTER 2: DISTINCT NEURAL CIRCUITS UNDERLIE PROSPECTIVE AND CONCURRENT MEMORY-GUIDED DECISION MAKING

The past is the best predictor of the future. This simple postulate belies the complex neurobiological mechanisms which facilitate an individual's use of memory to guide decisions. Previous research has shown that integration of memories bias decision making. Alternatively, memories can prospectively guide our choices. Here, the mechanisms and timing of the hippocampal (HPC), medial prefrontal (mPFC), and striatal contributions during prospective memory-guided decision making were elucidated. An associative learning task was developed in which the choice was conditional on the preceding stimulus. Two distinct networks emerged: (1) a prospective circuit consisting of the HPC, putamen (PUT), mPFC, and other cortical regions, which exhibited increased activation preceding successful conditional decisions; and (2) a concurrent circuit comprised of the dorsal anterior caudate (DAC), dorsolateral prefrontal cortex (dlPFC), and additional cortical structures that engaged during execution of correct conditional choices. These findings demonstrate distinct neurobiological circuits through which memory prospectively biases decisions and influence choice execution.

This chapter has been published in Cell Reports (Hamm & Mattfeld, 2019).

2.1 INTRODUCTION

Successful decision making often requires drawing upon the past. The influence of memory on decision making has been documented across a diverse array of tasks (Bornstein et al., 2017; Gluth et al., 2015; Jadhav et al., 2012; Murty et al., 2016; J. P. O'Doherty et al., 2017; Pfeiffer & Foster, 2013; Shohamy & Daw,

2015; Weber et al., 1993; Wimmer & Shohamy, 2012; Zeithamova, Schlichting, et al., 2012). Much of this research has examined "retrospective-integration" (Shohamy & Daw, 2015) or how experiences containing overlapping content are recalled, combined, and ultimately bias our future choices (Gluth et al., 2015; Murty et al., 2016; Wimmer & Shohamy, 2012; Zeithamova, Dominick, et al., 2012; Zeithamova, Schlichting, et al., 2012; Zeithamova & Preston, 2010). Yet, memories can also prospectively guide our choices. The neural mechanisms of how memory prospectively biases our decisions and the timing of those contributions remain central questions.

Memory of our intentions to act in the future, known as prospective memory, has demonstrated the influence of memory on subsequent behavior (Brandimonte et al., 1996; Kvavilashvili, 1987). Most research has focused on strategic monitoring and maintenance of prospective memory cues and have implicated the rostral prefrontal cortex (rPFC; BA10) as an important region for this process (Benoit et al., 2012, 2012; Burgess et al., 2003; Gilbert et al., 2005a; Gilbert, 2011; Haynes et al., 2007; Momennejad & Haynes, 2013; Okuda et al., 2007; Simons et al., 2006; Soon et al., 2008; Volle et al., 2011).

Less research has been devoted to the neurobiological mechanisms which support encoding prospective memory (Cona et al., 2015; Gilbert, 2011; Momennejad & Haynes, 2013); however, some computational work suggests prospective memory emerges from interactions between the prefrontal cortex and hippocampus (HPC), with the latter responsible for encoding associations between action plans and the context in which they are to take place (Cohen & O'Reilly,

1996). Research in rodents using spatial tasks strongly supports the role of the HPC through prospective neural signals (Benchenane et al., 2010; Euston et al., 2012; Jadhav et al., 2012; Pfeiffer & Foster, 2013; Shin & Jadhav, 2016; Wang & Morris, 2010; Yu & Frank, 2015). Based on the ability of the HPC to rapidly acquire relational representations (Eichenbaum & Cohen, 1988; Squire et al., 2004), contribute to future thinking (Addis et al., 2007; Schacter et al., 2017), and support prospective neural coding (Ferbinteanu & Shapiro, 2003), one would expect HPC activations to contribute to prospective memory-guided behavior.

In addition to area BA10, other regions of the medial prefrontal cortex (mPFC) likely contribute to mechanisms of prospective memory, owing in part to structural/functional diversity (de la Vega et al., 2016). While prospective memory paradigms have shown medial rPFC activations reflect ongoing task but not delayed intentions (Benoit et al., 2012; Burgess et al., 2003, 2011; Gilbert et al., 2005a; Simons et al., 2006), functional decoding analyses have identified additional mPFC regions related to storing of delayed intentions (Gilbert, 2011; Haynes et al., 2007; Momennejad & Haynes, 2013; Soon et al., 2008). Additionally, involvement of mPFC in maintenance of long-term memories (Bonnici et al., 2012; M. T. van Kesteren et al., 2010), integration of memories across episodes (Zeithamova & Preston, 2010), inferential decisions (Zeithamova, Schlichting, et al., 2012), and anatomical connections with the hippocampus and pre- and primary motor cortex (Barbas & Blatt, 1995; Cavada, 2000; Heidbreder & Groenewegen, 2003; Hoover & Vertes, 2007), all suggest the mPFC is well suited to use memory to guide behavior. Further, research in awake behaving rodents has identified

interactions between the HPC and mPFC related to memory-guided behavior (Benchenane et al., 2010; Jadhav et al., 2016; Shin & Jadhav, 2016), which are prominent during learning (Tang et al., 2017). Thus, I expect both activations in the mPFC, and its interactions with the HPC, should contribute to prospective memory.

The striatum, also important for decision making, supports action-selection (Balleine et al., 2007). Striatal activity (Tremblay et al., 1998) represents motor preparation, reward expectation, and prediction error (Schultz et al., 2003), all uniquely contributing to instrumental behavior, both response-outcome (goal-directed) and stimulus-response (habitual) (Graybiel, 1995; Liljeholm & O'Doherty, 2012; Yin et al., 2005). Notably, prospective memory paradigms rely on stimulus-response associations between prospective cues and specific actions (Beck et al., 2014; Einstein & McDaniel, 2005). Taken together, these findings suggest the striatum supports, not only prospective biasing of our choices, but also execution of those decisions.

The extent to which the HPC, mPFC, and striatum prospectively contribute to memory-guided conditional behavior in humans, as well as the timing of each, has not been demonstrated. Evidence from statistical learning studies have shown predictive activations in the HPC (Bornstein & Daw, 2012; Schapiro et al., 2012), while the mPFC is engaged during events sharing temporal associations (Schapiro et al., 2013). Prospective activations have also been identified in functionally decodable regions of the visual pathway during a multistep reward learning task (Doll et al., 2015). Striatum activation, specifically in the putamen, has been

associated with response preparation and prediction error using similar tasks (Bornstein & Daw, 2012; Doll et al., 2015).

A visuomotor associative learning paradigm (Law et al., 2005; Petrides, 1997) was designed to investigate how the HPC, mPFC, and regions of the striatum (dorsal anterior caudate and putamen) contribute to memory-guided behavior, both before and during conditional decision-making. Participants learned, through trial and error, to associate three stimuli with specific responses. Two images were *fixed* trials, whose associations were consistent across all presentations. For the third image, or *conditional* trial, correct response was dependent on the identity of the preceding trial stimulus. In other words, the correct association for the third image was *conditional* on the previous *fixed* association (Figure 1A-C). All learning stimuli were presented 80 times across two runs (40 trials/run). A total of three sets of stimuli were learned. Trials lasted three seconds and were as follows: (1) a central fixation cross [700 ms]; (2) followed by a kaleidoscopic image and two flanking boxes, during which participants make their selection [1000 ms]; and (3) participants were provided feedback (green “Yes!” if correct, red “No!” if incorrect, and white “?” if a response was not received in time) [800 ms]. All participants were given instructions of the task and received training outside of the scanner with a set of three unique training images.

With this approach, I investigated the mechanisms of memory-guided behavior. Two distinct neurobiological circuits emerged: one through which prospective memories are encoded and subsequently bias conditional memory-guided decisions, and a second which directs execution of concurrent choice.

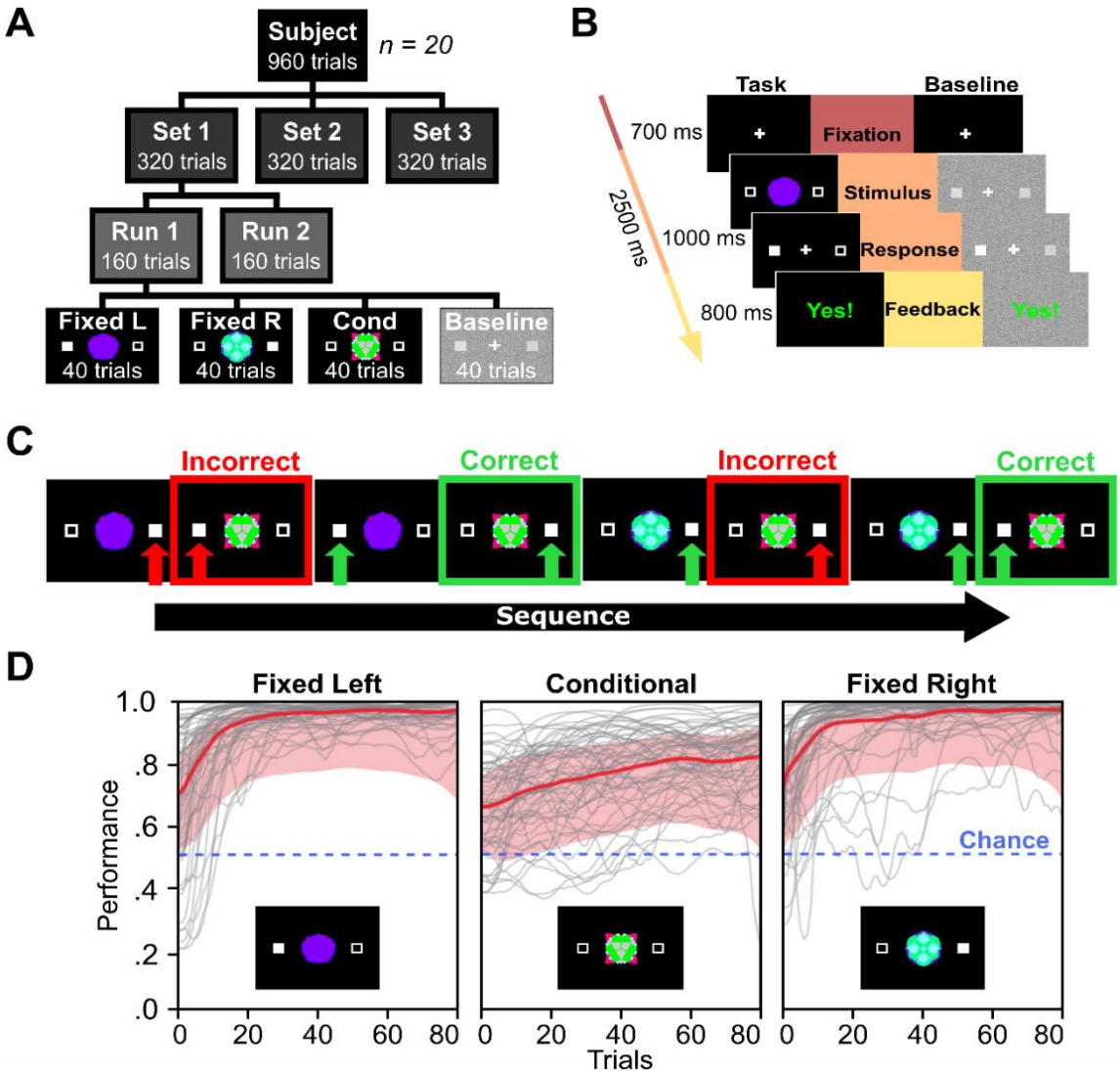

Figure 1. Schematic diagram of vCAT1 experiment and behavioral results.
(A) Each subject completed a total of 960 trials – comprised of three unique stimulus image sets of 320 trials each. Sets were further divided into two runs of 160 trials: 40 presentations of each trial type per set. (B) Task and baseline trial were identical in timing (2.5 sec) and structure. (C) Example sequence of events highlighting correct (green arrows/boxes) and incorrect (red arrows/boxes) responses for both fixed and conditional trials. (D) Performance curves were calculated for each participant across all image sets, producing a total of 60 unique curves. Performance was defined as the probability of a correct response on the respective trial. Dark red lines represent the mean curve for each stimulus type, while the surrounding pink expanse indicate the upper and lower bound 95% confidence intervals. Blue dashed line indicates chance performance of 50%.

2.2 METHODS

Twenty-seven right-handed volunteers performed a conditional visuo-motor associative learning task in the scanner. All participants provided written informed consent in accordance with local Institutional Review Board requirements. Individuals were recruited from the Florida International University community and financially compensated for their time. Six individuals were excluded from the reported analyses. Three were removed for excessive motion (greater than 20% of time points were flagged as outliers following outlier detection procedures using 1 mm normalized frame-wise displacement and three standard deviations above the mean signal intensity as thresholds). Three subjects were removed for poor task performance (lower bound of the 95% confidence interval never exceeded chance performance). Lastly, one participant was removed because of experimenter error – the first image set was erroneously presented for all six runs. The final sample size was 20 participants (13 females; mean age = 20.82 years, SD = 1.78).

2.2.1 BEHAVIORAL PROCEDURES

The conditional memory-guided associative learning task was modified from a visuomotor associative learning task (Law et al., 2005; Mattfeld & Stark, 2011, 2015; Stark et al., 2018). The experiment was run using PsychoPy2 software (version 1.81.02; (Peirce, 2009) on a Dell PC computer (Windows 8). Stimuli were back projected and viewed using a fixed mirror mounted on the head coil. Participants were presented with three unique kaleidoscopic image sets. Each set was learned across two scanning runs, comprising a total of six scanning runs.

Each run lasted 6.67 minutes. Images were presented 40 times during each run, or 80 times total across two runs, resulting in 240 learning stimulus trials per set. Individuals were instructed to learn through trial-and-error the associations between each image and one of two concurrently presented boxes, which flanked the stimulus. Two of the three images were associated with either the left or right box exclusively, for which the correct response remained consistent across trials. These trials as hereafter referred to as *fixed* associative learning trials. The association for the third image, however, was conditional on the identity of the image from the preceding trial and thus could change across trials. I refer to these trials as *conditional* associative learning trials (**Error! Reference source not f ound.**).

Each learning trial (3000 ms duration) began with the presentation of a centrally located fixation cross for 300 ms, after which a computer-generated kaleidoscopic image (Miyashita et al., 1991) flanked by empty boxes on both the right and left was presented for 500 ms. The image was then replaced by a fixation cross for a hold period of 700 ms, followed by a white “Go!” response cue and an additional 700 ms response window for participants to make their selection. Responses were registered by pressing with either the index (*Button 1 - indicating left box*) or the middle finger (*Button 2 - indicating right box)* using an MR-compatible response box. The selected box was highlighted to indicate selection. Deterministic feedback (green “Yes!”, red “No!”, or white “?”) was provided for 800ms post-response.

To serve as a temporal jitter between trial types, distribute cognitive demand, and provide a reference for the fMRI signal, 40 perceptual baseline (*BL*) trials were presented randomly across each experimental run. Sequence and timing of perceptual BL trials was identical to learning trials (Figure 1B). During BL trials, participants were presented with a random static image created through binarization of random values for each pixel of screen resolution (1280 x 800). Randomly generated pixel values greater than 0.85 became white, while those below threshold became gray. A white fixation cross between two white outlined boxes was presented at the center of the screen over the static background. In identical fashion to the underlying static image, contents of each box were also random patterns (320 x 200); however, the binarization threshold to produce a white pixel was considerably lower and, for target, vacillated as a function of performance. For the first BL trial, binarization thresholds for target and foil were initially set at 0.55 and 0.65, respectively. Participants were asked to identify which of the two boxes was “whiter”. If the participant responded correctly to seven out of the previous 10 trials, the white threshold for target box would increase by 10% of last trial, producing fewer white pixels and bringing the image closer to the constant foil threshold of 0.65, thereby increasing difficulty. Conversely, if response to fewer than five of the preceding 10 BL trials were correct, threshold decreased by 10% of previous trial value, resulting in a “whiter” target and easier identification.

2.2.2 PRESCAN TRAINING

All participants received prescan training of 75 total trials (60 learning stimuli and 15 BL trials) using a practice set of 3 images specific to the training session.

Prescan training allowed participants an opportunity to become acquainted with the nature and timing of the task and mitigated loss of trials due to nonresponse at the beginning of the first experimental run. Prescan training was conducted on a MacBook Pro using identical finger-response mapping used during scanning session.

2.2.3 MRI METHODS

Imaging data were acquired on a General Electric Discovery MR750 3T scanner (Waukesha, WI, USA) with a 32-channel head coil at the University of Miami Neuroimaging Facility (Miami, FL). Functional images were obtained using a T2*-sensitive gradient echo pulse sequence (42 interleaved axial slices, acquisition matrix = 96 x 96 mm, TR = 2000 ms, TE = 25 ms, flip angle = 75°, in-plane acquisition resolution = 2.5 x 2.5 mm, FOV = 240 mm, slice thickness = 3 mm). For each experimental run, 200 whole brain volumes were acquired. Acquisition of imaging data began after the fourth volume to permit stabilization of the magnetic resonance signal. A high-resolution, three-dimensional magnetization-prepared rapid gradient echo sequence (MP-RAGE) was collected for the purposes of coregistration and normalization (186 axial slices, voxel resolution = 1 mm isotropic, acquisition matrix = 256 x 256 mm, TR = 9.184 ms, TE = 3.68 ms, flip angle = 12°, FOV = 256 mm).

Data were preprocessed and analyzed using the following software packages: Analysis of Functional Neuroimages (AFNI version 16.3.18; Cox, 1996), FMRIB Software Library (FSL version 5.0.8; Jenkinson, Beckmann, Behrens, Woolrich, & Smith, 2012; Smith et al., 2004) Advanced Normalization Tools (ANTs

version 2.1.0; Avants et al., 2008), and Neuroimaging in Python (Nipype version 1.0.0.dev0; Gorgolewski, 2016) pipeline. T1-weighted structural scans underwent cortical surface reconstruction and cortical/subcortical segmentation. Surface reconstruction was visually inspected and errors were manually edited and resubmitted. Functional data were first 'despiked' removing and replacing intensity outliers in the functional time series. Simultaneous slice timing and motion correction (Roche, 2011) were performed, aligning all functional volumes to the middle volume of the first run. An affine transformation was calculated to co-register functional data to their structural scan. Motion and intensity outlier timepoints (>1 mm frame-wise-displacement; >3 SD mean intensity) were identified. Functional data were spatially filtered with a 5 mm kernel using the *SUSAN* algorithm (FSL; Smith & Brady, 1997), which preserves the underlying structure by only averaging local voxels with similar intensities. The last three volumes of each run were removed to eliminate scanner artifact observed during preprocessing.

Anatomical images were skull-stripped and then registered to the MNI-152 template (Fonov et al., 2009, 2011) via a rigid body transformation (FSL FLIRT; DOF = 6). This step was used to minimize large differences in position across participants and generate a template close to a commonly used reference. ANTs (Avants et al., 2008) software was used to create a study-specific template to minimize normalization error for any given participant. Each participant's skull-stripped brain was normalized using the non-linear symmetric diffeomorphic mapping implemented by ANTS. The resulting warps were applied to contrast

parameter estimates following fixed-effects modeling for subsequent group-level tests.

2.2.4 ANATOMICAL REGIONS OF INTEREST

Six anatomical regions of interest (ROIs) were bilaterally defined using each participant's structural scan. The hippocampus, putamen, and pre/primary motor cortex (precentral, paracentral, caudal middle frontal, and opercularis labels) were defined by binarizing segmentations from FreeSurfer aparc+aseg.mgz files. The mPFC was also defined using FreeSurfer segmentation (rostral and caudal anterior cingulate labels). Definition of the mPFC was limited to the anterior-most portion of the anterior cingulate cortex (ACC); admittedly, while ventral mPFC also receives input from the hippocampal formation, this region was not included due to substantial MRI signal drop-out. The dorsolateral prefrontal cortex (dlPFC) was defined using the Lausanne Atlas. The dorsal anterior caudate was manually segmented in accordance with anatomical landmarks outlined in the Atlas of the Human Brain (Mai et al., 1997): the appearance and secession of the anterior commissure defined the rostral boundary, while the lateral ventricle served as the medial edge and the internal capsule formed the lateral surface. All masks were back projected to functional space for analysis.

2.2.5 TASK-BASED FMRI DATA ANALYSIS

Collected fMRI data were analyzed using FSL, based on principles of the general linear model. Two separate univariate models at the first level were used to evaluate memory-guided conditional behavior. All models included regressors of no interest which included: motion parameters (x, y, z translations; pitch, roll,

yaw rotations), first and second derivatives of motion parameters, normalized motion, first, second, and third order Lagrange polynomials, as well as each outlier time-point exceeding artifact detection thresholds. For Model 1, the two regressors of interest consisted of fixed trials which immediately preceding (1) correct conditional trials or (2) incorrect conditional trials. All other trial types (i.e., conditional, fixed trials that preceded fixed trials, and fixed trials that preceded baseline trials, baseline trials) were modeled as a single regressor. Contrasts examined differences in activation between fixed trials preceding correct versus incorrect conditional trials. Model 2 included regressors of interest for (1) correct fixed trials, (2) incorrect fixed trials, (3) correct conditional trials, and (4) incorrect conditional trials. The contrast of interest for Model 2 was differences in activation for correct conditional versus correct fixed trials. Event regressors were convolved with FSL's double gamma hemodynamic response function whose onset coincided with stimulus presentation, and 2.5 seconds duration. Following first-level analyses, fixed-effects analyses across experimental runs were performed for each participant. Contrast parameter estimates from fixed-effects analysis were normalized to study specific template, and group-level analyses were performed using FSL's *Randomise* threshold-free cluster enhancement (tfce) one sample t-test ($p<0.05$).

2.2.6 BETA SERIES FUNCTIONAL CONNECTIVITY ANALYSIS

A beta-series correlation method (Rissman et al., 2004) was used for the task-based functional connectivity analysis. A least-squares single (LSS) approach (Mumford et al., 2012) was employed, given the fast event-related design. Briefly,

a separate general linear model was run for each trial of interest. All first level models included a regressor for the single relevant trial and all remaining task and nuisance regressors with relevant trial removed from its respective task regressor. Trials of interest were defined by whether they preceded periods of learning or non-learning for conditional trials. A logistic regression algorithm (Smith & Brown, 2003; Smith et al., 2004; Wirth et al., 2003) designed to assess learning as a dynamic process observed across trials was implemented to create unique learning curves for each conditional stimulus (MathWorks, 2012). Utilizing binary responses (correct/incorrect), learning state process was calculated from observed outcome of all experimental trials and served to indicate the probability of a correct response for any given trial, providing a metric of learning at each timepoint of the experimental run. Learning state was defined by obtaining the first derivative of the learning curve for conditional stimuli. If derivative value of the trial was positive, indicating an increase in the probability of being correct relative to the previous trial, then it was labeled a learning trial. If the value was less than or equal to zero, representing a decrease or no change in performance, then the trial was labeled as a non-learning trial. Fixed trials preceding learning and non-learning conditional trials were separately modeled and constructed into beta-series. *A priori* regions of interest were defined and average beta-series from each region were correlated with one another. The functional coupling during learning versus non-learning periods was quantified by degree to which the respective beta-series correlated.

2.3 RESULTS

To examine how HPC, mPFC, and subregions of the striatum (DAC and PUT) contribute to memory-guided behavior, blood oxygen level dependent (BOLD) functional magnetic resonance imaging (fMRI) was collected while participants engaged in a memory-guided conditional associative learning task. Anatomical region of interest (ROI) and exploratory whole-brain analyses tested: 1) differences in prospective activation during fixed trials immediately preceding correct compared to incorrect conditional trials, to evaluate neurobiological mechanisms of memory's influence on conditional decisions; 2) correlations between first trial regional activation and second trial performance for sequential fixed trial pairs when the stimulus either changed or remained the same, to further validate whether prospective activations bias subsequent behavior; 3) prospective functional coupling between anatomically connected regions of interest during periods of learning compared to periods of no-learning, to corroborate a recent study in rodents that found enhanced functional coupling during learning (Tang et al., 2017); and 4) activation differences between correct conditional and correct fixed association trials, to examine differences in brain activations for trials when conditional action was selected.

2.3.1 BEHAVIORAL PERFORMANCE

Participants were quicker and more accurate on fixed compared to conditional trials, and both were performed better than chance. For distributions that violated assumptions of parametric methods (i.e. accuracy and onset of learning), non-parametric Wilcoxon Signed-Rank and Friedman tests were

performed. All results were Bonferroni corrected for multiple comparisons where appropriate. To determine whether participants performed better than chance, median accuracy was calculated across stimulus sets for each participant. Participants demonstrated significantly better than chance performance for the fixed-right (FixR: median = 0.943, IQR: 0.926 – 0.958; FixR vs. chance: Z = -3.920, p < .0001), fixed-left (FixL: median = 0.928, IQR = 0.91 - 0.945; FixL vs. chance: Z = -3.921, p < .0001), and conditional images (Conditional: median = 0.77, IQR: 0.715 – 0.803; Conditional vs. chance: Z = -3.920, p < .0001). When comparing performance across trial types (FixR vs. FixL vs. Conditional), a significant difference for accuracy was observed ($\chi 2(2)$ = 31.013, p < .0001). To determine whether unexpected mnemonic differences exist between fixed-left and fixed-right trials, accuracies were compared. No significant difference between fixed-left and fixed-right trials was observed (Z = -1.248, p = .212). Given the consistent association between stimuli and response for fixed trials, I expected higher accuracy compared to conditional trials. Participants performed significantly better for both fixed-left (Z = -3.920, p < .001) and fixed-right (Z = -3.920, p < .001) compared to conditional trials. A statistically significant difference was observed for response time between the three trial types ($F(2,38)$ = 29.22, p < .0001, partial $\eta 2$ = .61). Fixed-left (0.580 s ± 0.008) and fixed-right (0.588 s ± 0.011) trials did not significantly differ ($t(19)$ = -1.086, p = .291). However, participants were significantly slower for conditional (0.632 ± 0.009) compared to either fixed-left ($t(19)$ = -9.429, p < .001) or fixed-right ($t(19)$ = -5.006, p < .001) trials. To assess whether conditional performance was related to the depth of processing during

fixed trials, I examined if response time for fixed trials varied as a function of conditional performance. Response times of fixed trials preceding correct conditional trials were not significantly different from fixed trials preceding incorrect conditional trials ($t(19) = .24$, $p = .81$).

Next, onset of learning for conditional trials was delayed compared to fixed association trials. To evaluate differences in learning between the three stimuli, learning curves with a logistic regression algorithm designed to assess learning as a dynamic process across trials were calculated (Figure 1C; Smith & Brown, 2003; Smith et al., 2004; Wirth et al., 2003). Differences in onset of learning between fixed and conditional trials were examined. The onset of learning was defined as the trial in which the lower-bound 95% confidence interval exceeded chance performance. There was a statistically significant difference in onset of learning between the three trial types ($\chi 2(2) = 22.354$, $p < .001$). The onset of learning for fixed-left (median = 3.835, IQR = 2 - 7) and fixed-right (median = 3.833, IQR = 1 - 7) trials was not significantly different ($Z = -0.081$, $p = .936$). In contrast, the onset of learning was delayed for conditional (median = 11.5, IQR = 6 - 26), compared to fixed-left ($Z = -3.267$, $p = .001$) and fixed-right ($Z = -3.435$, $p = .001$) trials.

In summary, no statistically significant differences were observed for accuracy, reaction time, or learning onset between fixed-left and fixed-right trials. Participants, however, were slower to respond, less accurate, and exhibited a delay in learning onset for conditional trials compared to fixed trials. All trial types were performed significantly better than chance.

2.3.2 PROSPECTIVE ACTIVATIONS OF HPC AND PUT, BUT NOT MPFC AND DAC, DIFFERENTIATE CONDITIONAL TRIAL PERFORMANCE

Success on conditional trials required participants to remember which of two fixed stimuli had been presented on the preceding trial. I anatomically defined regions of interest bilaterally (HPC, ACC, anterior dorsal caudate, and putamen; see STAR Methods) and contrasted level of activation on fixed trials immediately preceding correct and incorrect conditional trials. I predicted HPC, ACC, and anterior dorsal caudate would exhibit greater prospective activations preceding correct, compared to incorrect, conditional trials given their contributions to relational memory, memory integration, and flexible goal-directed behavior respectively. In contrast, I expected the putamen to play less of a prospective role.

The HPC and putamen, but not ACC and anterior dorsal caudate, prospectively differentiated successful conditional memory-guided behavior. Increased HPC activation was observed during fixed trials immediately preceding correct, compared to incorrect, conditional trials (Figure 2A; $t(19) = 3.275$, $p = .004$, $d = .63$). No significant difference in ACC (Figure 2B, $t(19) = 0.815$, $p = .42$) or anterior dorsal caudate (Figure 2C; $t(19) = -1.509$, $p = .15$) activation was observed for fixed trials before correct and incorrect conditional trials. Contrary to my hypothesis, greater putamen activation was observed during fixed trials before correct, relative to incorrect, conditional trials (Figure 2D; $t(19) = 3.247$, $p = .004$, $d = .57$).

To ensure these findings were not simply a performance artifact from the preceding fixed trial, the same analysis was conducted limiting scope to correct fixed trials preceding correct and incorrect conditionals. Again, both HPC (Figure S1A; $t(19) = 4.319$, $p = .0004$, $d = .88$) and putamen (Figure S1D; $t(19) = 2.565$, $p = .02$, $d = .59$) exhibited significantly greater activation during fixed trials preceding correct, compared to incorrect, conditional trials. No significant differences in the ACC (Figure S1B; $t(19) = 2.059$, $p = .05$) or dorsal anterior caudate (Figure S1C; $t(19) = 0.339$, $p = .74$) activations were observed.

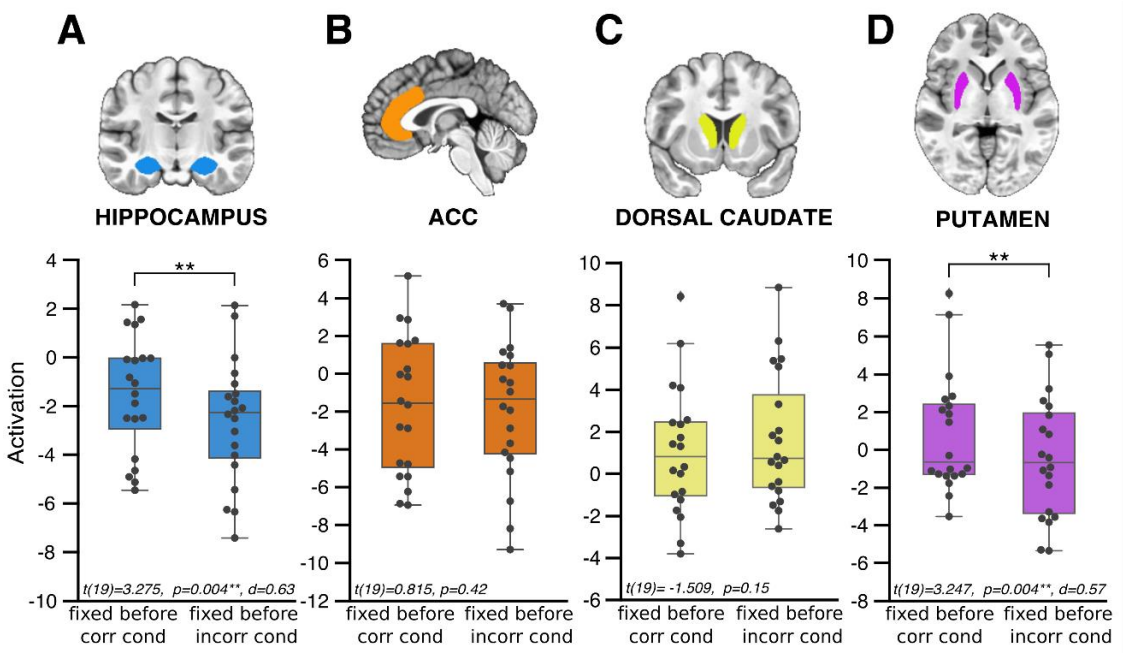

Figure 2. Prospective activations of the HPC and PUT, but not mPFC and DAC, differentiate conditional trial performance. Anatomical regions of interest included the: (A) hippocampus, (B) medial prefrontal cortex, (C) dorsal anterior caudate, and (D) putamen. Boxplots with overlaid swarm plots represent the activations for fixed trials preceding correct (corr cond) and incorrect (incorr cond) conditional trials. Significantly greater activation was observed in the (A) hippocampus and (D) putamen during fixed trials that preceded correct compared to incorrect conditional trials. See also Figure S1.

To provide further mechanistic insight into the nature of prospective signaling in the HPC and putamen, I compared activations for correct-only fixed-left, fixed-right, and conditional trials. If HPC and putamen contribute to either an encoding or prospective signal, I would expect to observe greater activations in these regions for fixed trials compared to conditional trials. In contrast, if conditional trial performance is dependent on retrieval-related mechanisms, the opposite pattern (greater activation for conditional compared to fixed trials) should emerge. Activations between fixed and conditional trials were significantly different in HPC (Figure S2; $F(2,38) = 10.575$, $p = .001$, $\eta^2 = .358$). Simple effects analysis revealed significantly greater activation for both fixed-left (-1.103 ± .45) and fixed-right (-1.266 ± .46) compared to conditional (-1.882 ± .47) trials (p's < .007), while no significant difference was found between fixed-left and fixed-right ($t(19) = 0.935$, $p = .36$). No significant differences were observed for trial type (Figure S2; $F(2,38) = 0.211$, $p = .81$) in the putamen.

The results of the *a priori* anatomical ROI analysis support the conclusion that prospective HPC and putamen, but not ACC and dorsal anterior caudate, activations are related to successful conditional memory.

2.3.3 Prospective cortical and subcortical activations for successful memory-guided decision making

Motivated by the complexities of the conditional memory-guided task and null findings for the ACC –proxy for mPFC – an exploratory whole-brain analysis was performed to evaluate potential contributions of additional cortical and subcortical regions to successful conditional memory-guided behavior. I found

memory-guided behavior prospectively employs a broad network of cortical and subcortical regions to guide our choices. I searched for voxel-wise differences in activation during fixed trials preceding correct and incorrect conditional trials. I performed a one-sample t-test using FSL *Randomise* with threshold-free cluster enhancement (tfce) correction with a threshold of $p < 0.05$. Consistent with *a priori* anatomical ROI analysis, clusters along the entire longitudinal axis of HPC and putamen survived correction for multiple comparisons when contrasting greater activation for fixed trials preceding correct conditional trials against fixed trials preceding incorrect conditional trials (Table S1).

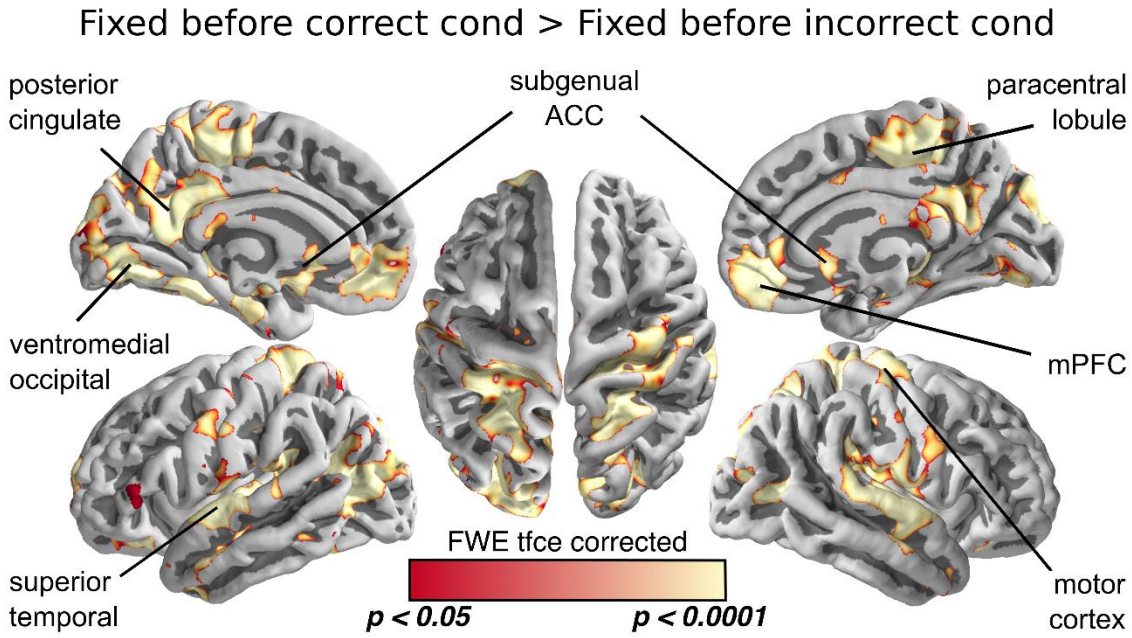

Figure 3. Prospective cortical activations for successful memory-guided conditional behavior. Cortical regions exhibiting greater activation for fixed trials before correct conditional (cond) trials > fixed trials before incorrect conditional (cond) trials following whole-brain exploratory analysis (FWE tfce corrected $p < 0.05$). Regions of activation included medial prefrontal cortex (mPFC), posterior cingulate cortex, superior temporal, motor cortex, ventromedial occipital, and the paracentral lobule.

Additional clusters were observed (Figure 3) for the same contrast in mPFC (paracingulate cortex extending into medial BA10 and subgenual ACC), posterior cingulate cortex (PCC) including the retrosplenial cortex, motor cortex, paracentral lobule, superior temporal cortex, ventral visual cortex, and the cerebellum (Figure S3). No regions survived correction for multiple comparisons when contrasting greater activation for fixed trials preceding incorrect conditional trials relative to fixed trials preceding correct conditional trials. These exploratory results suggest a widespread cortical and subcortical network prospectively bias conditional memory-guided decisions, including regions in mPFC notably anterior to anatomically defined ROI in the ACC.

2.3.4 PROSPECTIVE PUT ACTIVATION DURING FIXED TRIALS IS RELATED TO BEHAVIORAL PERFORMANCE ON SUBSEQUENT TRIALS WHEN IMAGE IS REPEATED

In addition to influencing decisions on conditional trials, prospective activations should also bias behavioral performance on subsequent fixed trials, especially when trials repeat. To evaluate the relationship between prospective fMRI activation and subsequent performance for fixed trials, temporally adjacent fixed trial pairs were selected and sorted according to whether stimuli changed (e.g., fixed-left → fixed-right) or remained the same (e.g., fixed-left → fixed-left). Using the same four *a priori* anatomical ROIs, Pearson's correlation coefficients were calculated between regional activation during the first trial and performance on the second. Betas were modeled separately for fixed trials followed by the same or different stimuli.

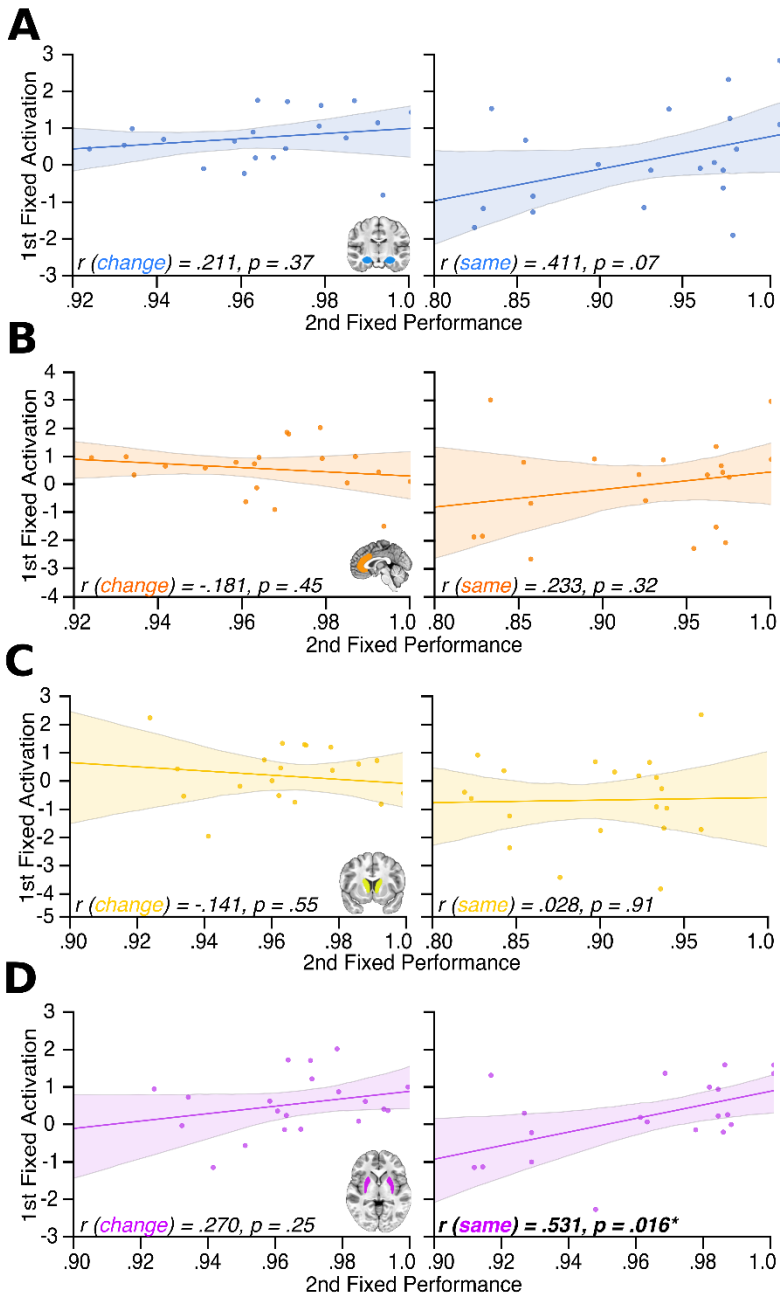

Figure 4. Prospective PUT activation during fixed trials is related to behavioral performance on subsequent trials when stimulus is repeated. Correlations between preceding fixed trial activation and subsequent fixed trial performance for same (e.g., fixed left → fixed left) and change (e.g., fixed left → fixed right) trial pairs. A trend was observed between activation in the hippocampus and fixed same pairs (A, right), while no significant relationship was observed in the same region for fixed-change pairs (A, left). No significant correlation between prior fixed activation and subsequent fixed performance was found for the (B) anterior cingulate cortex, or (C) dorsal caudate in either change or same pairs. A statistically significant positive correlation was found for the putamen on fixed same pairs (D, right), but not for fixed

Performance was defined as mean proportion of correct responses for trials that either remained the same (fixed-same) or changed (fixed-change). I expected fixed trial activations should be related to performance on upcoming fixed trials. To ensure these predictions were not a result of temporal adjacency, I compared activation for conditional trials to subsequent fixed trial performance.

PUT activation for preceding fixed trials was associated with behavioral performance of the following fixed trials when stimuli remained the same (Figure 4D, right; r = .535, p = .015, but not when changed (Figure 4D, left; r = .246, p = .30). No significant correlation was observed between HPC activation and performance for fixed-change trials (Figure 4A, left; r = .178, p = .45). However, a trend was observed for fixed-same trials (Figure 4A, right; r = .417, p = .07). No significant relationship between ACC activation and performance for fixed-change (Figure 4B, left; r = -.205, p = .39) nor fixed-same (Figure 4B, right; r = .343, p = .14) trials was found. No association between DAC activation and performance was observed for fixed-change (Figure 4C, left; r = -.161, p = .50) and fixed-same (Figure 4C, right; r = .063, p = .79) trials. Correlations were calculated between activations during conditional trials and following fixed trial performance. No significant relationship between conditional activation and subsequent behavioral performance was found (Figure S4A-D; all r < .22, all p > .05).

Consistent with my hypotheses, prospective fixed trial activations were associated with subsequent fixed trial behavioral performance in the putamen, while a trend was observed for HPC. In addition, no similar relationship was

identified when comparing conditional activations to upcoming fixed trial performance.

2.3.5 PROSPECTIVE HPC-MPFC FUNCTIONAL CORRELATIONS ARE ENHANCED DURING LEARNING

Functional coupling between *a priori* ROIs and known anatomically connected regions was examined. The HPC directly projects to ACC (Barbas & Blatt, 1995; Cavada, 2000); likewise, DAC and PUT receive projections from dorsolateral prefrontal cortex (dlPFC) and pre- and primary motor cortices, respectively (Flaherty & Graybiel, 1994; Haber, 2016; Haber et al., 2006; Künzle, 1975; McFarland & Haber, 2000; Selemon' & Goldman-Rakic, 1985).

To investigate how functional interactions between these regions support conditional memory-guided behavior, a task-based beta-series correlation analyses (Rissman et al., 2004) was performed. A recent study in rodents using an analogous task found increased coherence between the HPC and mPFC during learning relative to steady-state behavior (Tang et al., 2017). Thus, I examined functional coupling between three regional pairs during fixed trials preceding conditional trials for periods of learning and non-learning. To operationalize periods of *learning* and *non-learning*, the derivative of the learning curve was calculated across conditional trials. Trials with positive derivative values, representing an increase in performance relative to preceding trials, were considered *periods of learning*. Conversely, *periods of non-learning* were defined as trials in which the derivative was either zero or a negative value, constituting periods of stable or decreased performance. Separate beta-series were created using fixed trials

preceding learning and non-learning conditional trials, from which correlations between mean activations of anatomically defined ROIs were calculated.

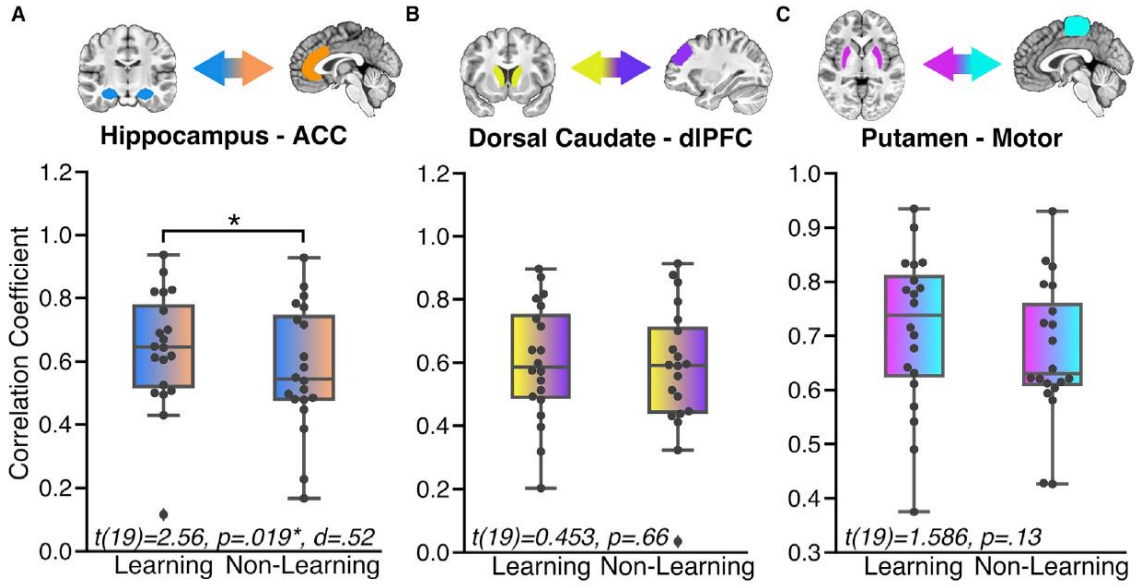

Figure 5. Prospective HPC-ACC functional correlations are enhanced during learning. Boxplots with overlaid swarm-plots represent distributions of correlations for periods of learning and non-learning between anatomically connected regions of interest. Paired-sample t-tests revealed only the hippocampus and anterior cingulate cortex (ACC) exhibited enhanced correlations as a function of learning. Dorsal lateral prefrontal cortex = dlPFC.

Functional coupling between the HPC and ACC was enhanced during periods of learning (positive derivative: 0.651 ± 0.041) relative to periods of non-learning (negative/zero derivative: 0.581 ± 0.044), $t(19) = 2.56$, $p = .019$, $d = .52$. Conversely, no differences in functional coupling were observed between periods of learning (0.588 ± 0.041) and non-learning (0.570 ± 0.045) for either DAC and dlPFC, $t(19) = 0.453$, $p = .66$, nor PUT and pre/primary motor cortex, $t(19) = 1.586$, $p = 0.13$ (Figure 5).

2.3.6 INTERVENING BASELINE TRIAL REPRESENTATIONAL DISSIMILARITY IN THE HPC AND MPFC DID NOT CORRELATE WITH BEHAVIORAL PERFORMANCE ON SUBSEQUENT CONDITIONAL TRIALS

To further elucidate mechanistic contributions of the HPC and mPFC to prospective memory-guided behavior, I used a multivariate approach to evaluate possible content of HPC and mPFC representations during baseline trials which fell between fixed and conditional trials. The HPC was anatomically delineated, while mPFC voxels were defined using a hybrid functional/anatomical mask. If activations in these regions reflected maintenance of relevant associations until conditional cue was presented, conditional performance should be enhanced when pattern dissimilarity between intervening baseline and preceding fixed trials was low. In other words, if the pattern of HPC or mPFC activation across voxels during intervening baseline trials was similar to the pattern during typical fixed preceding correct conditional trials, similarities may reflect the maintenance of information; thus, the degree to which such patterns shift would be predictive of impaired performance. I found no relationship between magnitude of pattern similarity for intervening baseline activations with fixed trials preceding correct conditional activations, and behavioral performance (Figure S5; HPC: $r = 0.092$, $p = 0.70$; mPFC: $r = 0.188$, $p = 0.43$).

2.3.7 SEPARATE NETWORK SUPPORTS SUCCESSFUL EXECUTION OF CONDITIONAL DECISION MAKING

I found execution of conditional associations is supported by a wide network of cortical and subcortical regions distinct from observed prospective activations. I performed a second exploratory whole-brain analysis to determine which regions contribute to successful memory-guided behavior during, rather than preceding, correct conditional associative trials. I compared differences in activation during correct conditional, compared to correct fixed, trials (Table S1). I observed greater activation for correct conditional trials in the bilateral caudate, dlPFC, superior parietal lobule (SPL), anterior insular cortex, and cerebellum (Figure 6).

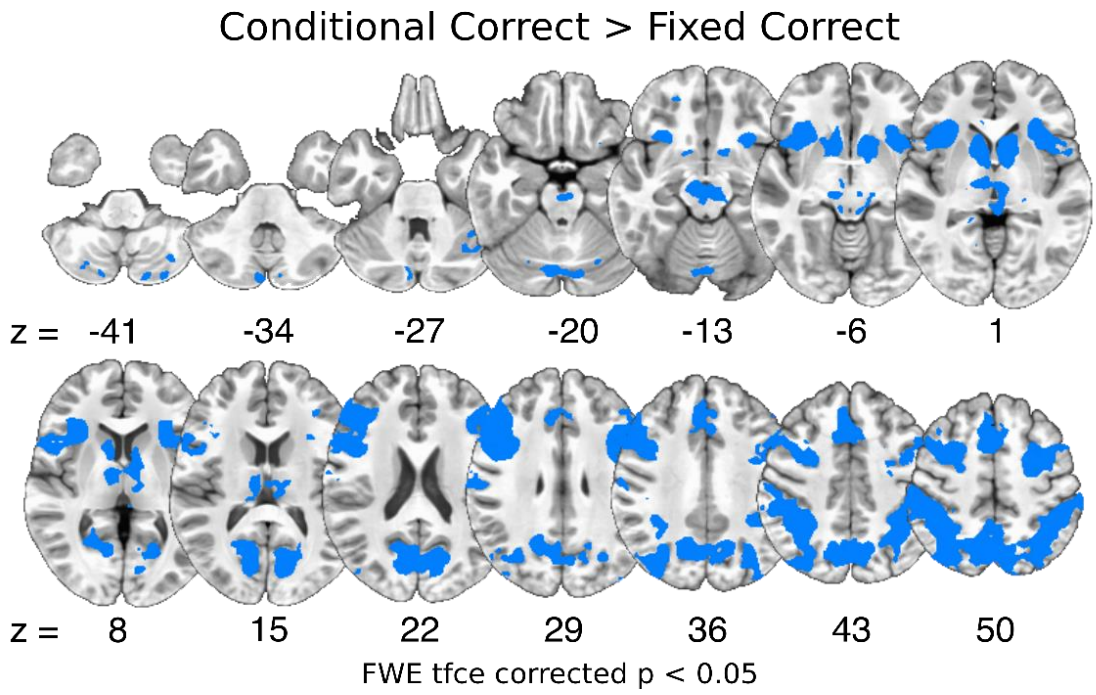

Figure 6. Separate network supports successful execution of current conditional decision. Cortical and subcortical regions exhibiting greater activation for correct conditional trials compared to correct fixed trials following a whole-brain exploratory analysis (FWE tfce corrected $p < 0.05$). Regions of activation included the bilateral caudate, dorsolateral prefrontal cortex, presupplementary motor area, anterior insula, superior parietal cortex, precuneus, and cerebellum.

These results reveal a separate network of brain regions important for concurrent conditional trial performance (e.g., action-selection) which contribute to the execution of conditional memory-guided behavior, above and beyond those implicated in preceding fixed trials.

2.4 Discussion

I investigated prospective memory-guided behavior using a conditional associative learning task. Success on conditional trials was dependent on the stimulus identity from the preceding fixed trial. Using a combination of univariate, multivariate, and connectivity analyses, I identified prospective activations in a network related to successful future decision-making. In addition, a second separate network associated with successful execution of conditional memory-guided behavior was discovered. These findings demonstrate memory-guided behavior is supported by two distinct neurobiological circuits: one dependent on the hippocampus, putamen, mPFC, and other cortical regions which prospectively bias subsequent conditional decisions; while the second relies on the striatum, dlPFC, and other cortical regions to use past knowledge for choice execution.

Prospective neural activity constitutes an important mechanism of memory-guided behavior. As expected, HPC activations during fixed preceding conditional trials differentiated conditional performance. Notably, in the current task, HPC is recruited for behavior with very short delays (3000 ms). Such findings may arise from the highly associative nature of the task, as similar hippocampal outcomes have been identified for relational tasks with short delays (Hannula & Ranganath, 2008), and reflect more temporally compressed contributions when prospective

mechanisms are engaged during deliberation (Redish, 2016). An exploratory whole brain analysis identified a broad network of cortical and subcortical regions with prospective activity, including subregions of the mPFC (paracingulate cortex extending into BA10 and subgenual ACC), posterior cingulate cortex extending into retrosplenial cortex, superior temporal cortex, paracentral lobule, and cerebellum. Surprisingly, the putamen exhibited a similar pattern in activation. The influence of activations in HPC and putamen were not limited to conditional decisions. I also identified a relationship between fixed trial activation and subsequent fixed trial performance in the putamen when stimuli were repeated. In the same analysis, a trend was also observed for HPC. To gain further insight into mechanistic contributions of HPC and mPFC, I followed my univariate analyses with a multivariate approach. I utilized pattern similarity analysis to determine whether content of fixed trials was maintained during interceding baseline trials. No evidence was found to support a relationship between behavioral performance on conditional trials following intervening baselines and representational similarity in either HPC or mPFC. The relationships between time, learning, and continuous measurement of performance constitute important limitations. While the motivating goal of this experiment was to elucidate neurobiological mechanisms of successful conditional memory guided behavior, these mechanisms may evolve with experience (see Chapter 3).

These results extend previous findings in both human and animal literature. Recent studies have identified relationships between prospective fMRI activations and choice. For example, in a study which used a multistep reward learning task

combined with regionally decodable stimuli, prospective activation of second-stage categories was positively correlated with the degree to which participants used a model-based, relative to a model-free, strategy (Doll et al., 2015). In a sequential learning task where regularity of adjacent items was manipulated, hippocampal activation correlated with forward entropy, an estimate of uncertainty of upcoming stimulus conditional on the current one (Bornstein & Daw, 2012). Lastly, hippocampal activations during encoding have been shown to correlate with probability an item was remembered during a later decision phase (Gluth et al., 2015). In the same studies, activations in putamen were associated with model-free prediction errors (Bornstein & Daw, 2012; Doll et al., 2015) and conditional probability, or degree of response preparation during a sequential learning task (Bornstein et al., 2017). Prospective neural activity constitutes a form of reactivation, which has long been thought to be an important retrieval-related mechanism (J. D. Johnson et al., 2009). In a recent action-based learning study, reactivations of the medial temporal lobe for stimulus triads linked by predictive actions were negatively correlated with stimulus-selective visual cortex activations (Hindy & Turk-Browne, 2016), suggesting expectations of predictive actions lessen the necessity of sensory processing. The HPC has also been shown to represent prospective rewards during a monetary incentive encoding task (Zeithamova et al., 2018), and prospective planning signals in the HPC were related to one-shot paired associate learning in a spatial task (van Kesteren et al., 2018). Spatial navigation studies in rodents have also provided evidence for the role of prospective neural activity for decision-making in the HPC. Awake sharp wave

ripple (SWR) events in HPC reinstate sequential patterns of ‘place-cell’ activity of both recent (Diba & Buzsáki, 2007; Foster & Wilson, 2006) and remote experiences (Gupta et al., 2010; Karlsson & Frank, 2009). Further, SWRs are predictive of upcoming choices (Pfeiffer & Foster, 2013), indicative of whether those choices will be subsequently correct or incorrect (Singer et al., 2013). Disruptions of these SWRs were sufficient to impair performance in a continuous alternation task (Jadhav et al., 2012). Here, I observed greater activation in HPC and putamen on trials which preceded correct versus incorrect conditional memory-guided trials, like both results observed in rodents during an analogous spatial alternation task (Frank et al., 2000; Singer et al., 2013) and statistical learning studies in humans (Bornstein & Daw, 2012). Altogether and framed within the larger literature, these results suggest HPC and other regions play an important role in how memory representations prospectively guide decision making.

The observed activations in this study may reflect a retrieval process important for deliberation at time of choice (Carr et al., 2011). Evidence suggests prospective activations reflect imagined future options important for upcoming decisions (Addis et al., 2007; Yu & Frank, 2015); however, research in prospective memory provides a compelling alternative. The investigation of prospective memory has been carried out within a multi-process framework, which posits prospective remembering is supported by either resource-demanding strategic monitoring or a spontaneous retrieval mechanism (Braver, 2012; McDaniel & Einstein, 2000). Which mechanism prevails is thought to be dependent on contextual features, such as task structure (Einstein & McDaniel, 2005; Scullin et

al., 2010). Many studies provide evidence for a neurobiological mechanism centered on the rPFC which supports strategic monitoring (Benoit et al., 2012; Burgess et al., 2003, 2011; Gilbert, 2011; Gilbert et al., 2005b; Momennejad & Haynes, 2013; Okuda et al., 2007; Simons et al., 2006).

For spontaneous retrieval, the hippocampal system would be expected to play an important role (Einstein & McDaniel, 2005). However, studies of transient responses to prospective memory-target stimuli have not demonstrated hippocampal activations (Beck et al., 2014; Reynolds et al., 2009). Rather, bilateral hippocampal activation was observed during encoding of prospective memory intentions (Gilbert, 2011). In the current study, activation in the HPC and other structures during fixed trials proceeding conditionals may reflect encoding of prospective memories. Such an interpretation would be consistent with computational models positing prospective memory results from interactions between prefrontal cortex and HPC, the latter responsible for encoding associations between action plans and future contexts (Cohen & O'Reilly, 1996).

Functional interactions between HPC and ACC constitute an important mechanism supporting memory-guided conditional behavior modulated by learning. I observed prospective functional coupling between HPC and ACC was enhanced during learning compared to non-learning. Similar differences were not found between either dorsal anterior caudate and dlPFC, or putamen and pre/primary motor cortex. Previous human neuroimaging studies have shown coupling between HPC and mPFC play a central role in memory-guided decision making (Gluth et al., 2015; Zeithamova, Dominick, et al., 2012), memory updating

and integration (Preston & Eichenbaum, 2013; Schlichting & Preston, 2016; M. T. van Kesteren et al., 2010), statistical learning of temporal community structure (Schapiro et al., 2016), and retrieval (King et al., 2015; Schedlbauer et al., 2014). Much work in humans has rested on the theory mPFC guides HPC encoding and retrieval (Preston & Eichenbaum, 2013). The results from this study extend these observations to show such interactions are modifiable through learning. Functional coupling between HPC and mPFC in awake behaving rodents has shown to be an important mechanism in memory-guided behavior (Benchenane et al., 2010; Brincat & Miller, 2015; Guise & Shapiro, 2017; Jadhav et al., 2016; Jones & Wilson, 2005a, 2005b; Remondes & Wilson, 2013; Tang et al., 2017; Yu & Frank, 2015). For example, coupling of spike-timing and theta coherence increases at choice points in mazes, with degree of coherence modulated by behavioral performance (Benchenane et al., 2010; Jones & Wilson, 2005a). I observed enhanced HPC-ACC coupling during learning relative to non-learning periods, similar to a recent rodent study (Tang et al., 2017). In this study, functional interactions between HPC and ACC may reflect a mechanism by which ACC modifies HPC activations to facilitate goal directed behavior. Such a possibility is in line with studies in rodents using a goal-directed paradigm (Guise & Shapiro, 2017).

Activations in dorsal anterior caudate and related cortical structures (e.g., dlPFC, superior parietal lobule, anterior insula, and precuneus) were associated with successful execution of conditional memory-guided behavior when compared to correct fixed association trials. The dorsal anterior striatum represents currently relevant associations of goal-directed behavior. The striatum has long been

believed to support instrumental behavior (Graybiel, 1995). Instrumental behavior is dissociable into goal-directed and stimulus-bound or habitual control (Dickinson & Balleine, 1994), with each having been mapped to different neurobiological circuits. Specifically, evidence from animal studies suggest goal-directed behavior is mediated by dorsomedial striatal circuits (Yin et al., 2005), while stimulus-bound behavior is supported by dorsolateral circuits (Yin & Knowlton, 2004). A similar functional subdivision is observed in primates along the anterior/posterior axis (Miyachi et al., 1997, 2002). Neurons in DAC modulate firing as goal-directed associations are learned (Blazquez et al., 2002; Brasted & Wise, 2004; Hadj-Bouziane et al., 2006; Miyachi et al., 2002; Tremblay et al., 1998), with preceding responses observed in the dorsolateral prefrontal cortex (Pasupathy & Miller, 2005). Similar activations have been observed in humans during instrumental tasks (O'Doherty et al., 2004; Tricomi et al., 2004). In prospective memory studies, associations between prospective memory cues and specific actions share many features with instrumental designs. Prior prospective memory studies have reported transient activations in response to prospective memory target cues across both cortical and subcortical regions, findings which largely overlap with regions identified in my current study (Beck et al., 2014; McDaniel et al., 2013; Reynolds et al., 2009; Simons et al., 2006). Thus, activation in the DAC and affiliated cortical structures for correct conditional greater than correct fixed associations reflect instrumental goal-directed associations at action selection.

2.5 CONCLUSIONS

Taken together, these findings provide evidence for complementary memory processes underlying successful conditional memory-guided behavior. I posit the first of these mechanisms to represent a prospective encoding system which serves to procure and maintain multiple types of representations across experience for future conditional decisions dependent on the HPC and related cortical structures. In addition, I propose a second conditional memory-guided system, reliant on the striatum and affiliated cortex, which facilitates concurrent use of past knowledge during choice deliberation. My findings illustrate successful conditional memory-guided decisions arise from the involvement of multiple learning and memory systems.

2.6 DATA AND CODE AVAILABILITY

The raw magnetic resonance imaging (MRI) datasets generated during this study are available at OpenNEURO.org (accession number: 10.18112/openneuro.ds002078.v1.0.0). The code supporting the current study has been deposited in a public repository on GitHub (https://github.com/madlab-fiu/wmaze).

CHAPTER 3: DISTINCT CONTRIBUTIONS OF THE HPC AND DAC TO MEMORY-GUIDED DECISION MAKING EVOLVE ACROSS LEARNING

3.1 INTRODUCTION

In the field of learning and memory research, most studies have focused on neural correlates of memory, with far less attention paid to how such memories evolve over experience. While research has examined specific regions and related networks supporting memory-guided decision making (Hamm & Mattfeld, 2019; Shin et al., 2019; Shin & Jadhav, 2016), how these neurobiological contributions develop across experience-based learning remains a fascinating, and important, question.

Two interconnected structures known to facilitate memory-guided behavior are the caudate nucleus (Balleine et al., 2007; Schultz et al., 2003; Tremblay et al., 1998; van der Meer et al., 2012) and hippocampus (Eichenbaum & Cohen, 1988; Squire et al., 2004). The caudate nucleus contributes to learning through modulation of activation to contingencies between behaviors and outcomes (Brovelli et al., 2011; Tricomi et al., 2004), planning of self-initiated novel action (François-Brosseau et al., 2009; Provost et al., 2010) and complex action sequences (Hamm & Mattfeld, 2019; Mattfeld & Stark, 2011; Owen et al., 1996), instrumental learning resulting from direct experience (Cooper et al., 2012) acquisition of visuomotor skills (Cavaco et al., 2011), adaptation toward successful behavioral action in reward-based tasks (Haruno & Kawato, 2006; Koch et al., 2008), flexibility in response behavior (Ragozzino, 2003), and prediction error (O'Doherty et al., 2004; O'Doherty et al., 2017). Animal and human research has

demonstrated the HPC plays a necessary role in spatial memory and navigation (Ego-Stengel & Wilson, 2010; Howard & Eichenbaum, 2015; Jadhav et al., 2012; Jones & Wilson, 2005b; Skinner et al., 2014), sequence memory (Allen et al., 2014, 2015; Jayachandran et al., 2019; Reeders et al., 2021), and conditional associative memory (Benchenane et al., 2010; Hamm & Mattfeld, 2019; Shin & Jadhav, 2016). However, many memory paradigms used in these studies utilize either single-event encoding or evaluate neurophysiology during steady-state performance following extensive periods of training. Few studies have focused on how HPC involvement changes across periods of learning on the scale of minutes.

The HPC and DAC has been implicated in memory-guided decision making via distinct networks which facilitate prospective encoding and choice deliberation/execution, respectively, using BOLD fMRI (Hamm & Mattfeld, 2019). The current study expands on the previous findings by investigating how distinct contributions of these regions change across learning.

Pattern similarity, and inversely, dissimilarity, analysis of fMRI data has been successfully used as a neurobiological metric of learning and shown to be predictive of successful retrieval processes (Hsieh et al., 2014; Qu et al., 2017; Xue et al., 2010). Therefore, I conducted a pattern dissimilarity analysis using first level, unsmoothed functional data, followed by fixed effect analyses to quantify dissimilarity of activation patterns during periods of early and late learning. A correlation analysis was performed to determine the relationship between pattern dissimilarity for periods preceding correct vs incorrect conditional trials and learning performance. I discovered increased pattern dissimilarity for late,

compared to early, learning for both HPC and DAC. Additionally, I found a significant positive correlation between pattern dissimilarity and learning performance for DAC during both early and late learning. However, for HPC, a significant positive relationship was only observed during late learning, and merely trended toward significance during early learning.

3.2 METHODS

Twenty right-handed volunteers (13 female, mean age = 20.82, SD = 1.78) at Florida International University were recruited to perform a conditional visuo-motor association learning task in a magnetic resonance imaging scanner. All participants provided written informed consent in accordance with local Institutional Review Board requirements. Individuals were recruited from the Florida International University community and financially compensated for their time. Six individuals were excluded from the reported analyses. Three were removed for excessive motion (greater than 20% of time points were flagged as outliers following outlier detection procedures using 1 mm normalized frame-wise displacement and three standard deviations above the mean signal intensity as thresholds). Three subjects were removed for poor task performance (lower bound of the 95% confidence interval never exceeded chance performance). Lastly, one participant was removed because of experimenter error – the first image set was erroneously presented for all six runs. The final sample size was 20 participants (13 females; mean age = 20.82 years, SD = 1.78).

3.2.1 BEHAVIORAL PROCEDURES

3.2.1.1 CONDITIONAL ASSOCIATIVE TASK #1 (vCAT1)

The task was modified from the visuomotor conditional associative learning task (Hamm & Mattfeld, 2019; Law et al., 2005; Mattfeld & Stark, 2011; Stark et al., 2018). Participants associated visual stimuli with one of two possible responses. Stimuli consisted of three computer-generated kaleidoscopic images, presented one at a time, and centered between two white boxes. Participants were asked to determine, through trial and error, the relationship between each kaleidoscopic image and one of two flanking boxes. Responses were registered by pressing with either an index (*Button 1 - indicating left box*) or middle finger (*Button 2 - indicating right box)* using an MR-compatible response box. Correct associations for two images were “fixed” and remained consistent across all presentations. Conversely, associated response for the third image was “conditional”, or dependent on the identity of the preceding fixed trial stimulus (Figure 7A). In other words, fixed trial images would always be associated with either the left or right box, while correct response to conditional trial images would change depending on which fixed association preceded. Learning trial (2500 ms total duration) consisted of three sequential phases: fixation, stimulus presentation and response, and feedback (Figure 7B). Each image was presented 80 times across two experimental runs (40 per run).

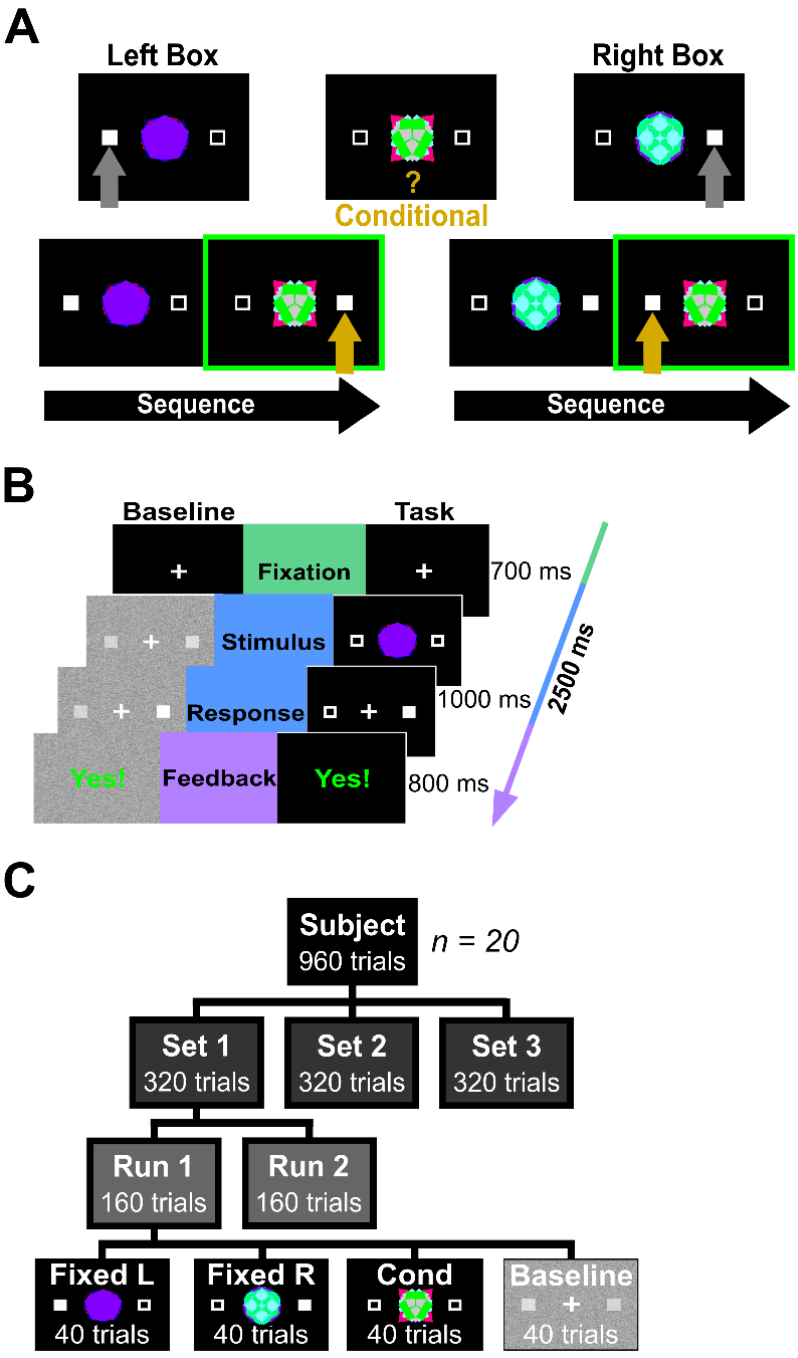

Figure 7. Schematic diagram of vCAT1 trial and experiment design. (A) Example of fixed and conditional trials, as well as fixed-conditional sequence. (B) Task and baseline trials were identical in timing (2.5 s) and structure. (C) Total number of trials across experiment categorized by sets, runs, and trial types.

Each participant learned associations for three sets of images for a total of 720 learning trials per participant (Figure 7C). Perceptual baseline trials (BL; 40 per run) were presented alongside learning trials. During these trials, participants were asked to select the “whiter” of two boxes. Inclusion of these BL trials served three purposes: temporal jitter between trial types, distribution of cognitive demand, and reference for fMRI signal. BL trials were identical to learning trials in sequence and timing.

3.2.2 PRE-SCAN TRAINING

All participants received prescan training of 75 total trials (60 learning stimuli and 15 BL trials) using a practice set of 3 images specific to the training session. Prescan training allowed participants an opportunity to become acquainted with the nature and timing of the task and mitigated loss of trials due to nonresponse at the beginning of the first experimental run. Prescan training was conducted on a MacBook Pro using identical finger-response mapping used during scanning session.

3.2.3 MRI METHODS

Magnetic resonance imaging data was collected on a General Electric Discovery MR750 3T scanner (Waukesha, WI, USA) with 32-channel head coil at the University of Miami Neuroimaging Facility (Miami, FL). Functional data was obtain using a T2*-sensitive gradient echo pulse sequence (42 interleaved axial slices, acquisition matrix = 96 X 96 mm, TR = 2000 ms, TE = 25 mm, flip angle = 75˚, in-plane acquisition resolution = 2.5 X 2.5 mm, FOV = 240 mm, slice thickness = 3 mm). Two hundred (200) whole-brain images were collected per

experimental run. For purposes of coregistration and registration, high-resolution three-dimensional magnetization-prepared rapid gradient echo sequence (MP-RAGE) was collected (186 axial slices, voxel resolution = 1 mm isotropic, acquisition matrix = 256 x 256 mm, TR = 9.184 ms, TE = 3.68 ms, flip angle = 12˚, FOV = 256 mm). Two anatomical regions of interest (ROIs) were bilaterally defined. The hippocampus was defined through binarization of Freesurfer segmentation files (aparc+aseg.mgz). The dorsal anterior caudate (DAC) was manually segmented in accordance with anatomical landmarks outlined in Atlas of the Human Brain (Mai et al., 2004): appearance and secession of anterior commissure defined rostral boundaries, while lateral ventricle served as medial edge and internal capsule formed the lateral surface.

Data were preprocessed and analyzed using the following software packages: Analysis of Functional Neuroimages (AFNI version 16.3.18; (Cox, 1996), FMRIB Software Library (FSL version 5.0.8; Jenkinson, Beckmann, Behrens, Woolrich, & Smith, 2012; Smith et al., 2004) Advanced Normalization Tools (ANTs version 2.1.0; (Avants et al., 2008), and Neuroimaging in Python (Nipype version 1.0.0.dev0; (Gorgolewski, 2016) pipeline. T1-weighted structural scans underwent cortical surface reconstruction and cortical/subcortical segmentation. Surface reconstruction was visually inspected and errors were manually edited and resubmitted. Functional data were first ‘despiked’ removing and replacing intensity outliers in the functional time series. Simultaneous slice timing and motion correction (Roche, 2011) were performed, aligning all functional volumes to the middle volume of the first run. An affine transformation was

calculated to co-register functional data to their structural scan. Motion and intensity outlier timepoints (>1 mm frame-wise-displacement; >3 SD mean intensity) were identified. Functional data were spatially filtered with a 5 mm kernel using the *SUSAN* algorithm (FSL; (S. M. Smith & Brady, 1997), which preserves the underlying structure by only averaging local voxels with similar intensities. The last three volumes of each run were removed to eliminate scanner artifact observed during preprocessing.

Anatomical images were skull-stripped and then registered to the MNI-152 template (Fonov et al., 2009, 2011) via a rigid body transformation (FSL FLIRT; DOF = 6). This step was used to minimize large differences in position across participants and generate a template close to a commonly used reference. ANTs (Avants et al., 2008) software was used to create a study-specific template to minimize normalization error for any given participant. Each participant's skull-stripped brain was normalized using the non-linear symmetric diffeomorphic mapping implemented by ANTS. The resulting warps were applied to contrast parameter estimates following fixed-effects modeling for subsequent group-level tests.

3.2.4 ANATOMICAL REGIONS OF INTEREST

Six anatomical regions of interest (ROIs) were bilaterally defined using each participant's structural scan. The hippocampus, putamen, and pre/primary motor cortex (precentral, paracentral, caudal middle frontal, and opercularis labels) were defined by binarizing segmentations from FreeSurfer aparc+aseg.mgz files. The mPFC was also defined using FreeSurfer segmentation (rostral and caudal

anterior cingulate labels). Definition of the mPFC was limited to the anterior-most portion of the anterior cingulate cortex (ACC); admittedly, while ventral mPFC also receives input from the hippocampal formation, this region was not included due to substantial MRI signal drop-out. The dorsolateral prefrontal cortex (dlPFC) was defined using the Lausanne Atlas. The dorsal anterior caudate was manually segmented in accordance with anatomical landmarks outlined in the Atlas of the Human Brain (Mai et al., 1997): the appearance and secession of the anterior commissure defined the rostral boundary, while the lateral ventricle served as the medial edge and the internal capsule formed the lateral surface. All masks were back projected to functional space for analysis.

3.2.5 TASK-BASED FMRI DATA ANALYSIS

Functional neuroimaging data were analyzed using FSL in accordance with the general linear model. One univariate model at 1st level was used to evaluate learning across early and late memory-guided conditional behavior. Regressors of interest included (1) fixed trials which proceeded correct conditional trials and (2) fixed trials which proceeded incorrect conditional trials. A second univariate model at 2nd level was used to determine how contributions of the HPC and DAC change across levels of performance. Regressor of interest included: conditional trials assigned to (1) Bin 1 or lowest 1/3 of performance, (2) Bin 2 or intermediate 1/3, and (3) Bin 3 or highest 1/3. For both models, regressors of no interest included motion parameters (x, y, z; pitch, roll, yaw), 1st and 2nd derivatives of motion parameters, normalized motion, 1st, 2nd, and 3rd order Lagrange polynomials, and outlier time-points exceeding artifact detection threshold. For the pattern

dissimilarity analysis, first-level analyses were performed on unsmoothed data for six experimental runs. Correlation values were calculated between voxel-wise patterns of analysis in anatomically defined ROIs (i.e., HPC and DAC) for fixed trials preceding correct versus incorrect conditional trials using Pearson's correlation coefficient (*r*). Pattern dissimilarity was subsequently defined using obtained correlation as 1-r. Learning was quantified using a logistic regression algorithm designed to assess learning as a dynamic process across trials, creating representative curves which provide participants' probability of a correct response for any given trial (Smith & Brown, 2003; Smith et al., 2004). For the binned learning analysis, first-level analyses were performed on smoothed data for six experimental runs. Following first-level analyses, fixed effects analyses across runs were performed for each participant for each respective contrasts of interest.

3.3 RESULTS

To examine how HPC and DAC contribute to memory-guided behavior across learning, I collected blood oxygen level dependent (BOLD) functional magnetic resonance imaging (fMRI) while participants engaged in a memory-guided conditional associative learning task. Binned learning curve and pattern dissimilarity analyses tested: (1) regional pattern dissimilarity for periods preceding correct compared to incorrect conditional trials, to determine whether contributions to prospective learning change from early to late learning, and (2) mean regional activations observed during conditional trial behavior across learning bins, to examine how regional activations develop with improved performance.

3.3.1 BEHAVIORAL PERFORMANCE

Participant performance exceeded chance for fixed-right (Fix_R: median = 0.943, IQR: 0.926 – 0.958; $Fix_{R\ vs.\ chance}$: Z = -3.920, p < .0001), fixed-left (Fix_L: median = 0.928, IQR = 0.91 - 0.945; $Fix_{L\ vs.\ chance}$: Z = -3.921, p < .0001), and conditional images (Conditional: median = 0.77, IQR: 0.715 – 0.803; $Conditional_{vs.\ chance}$: Z = -3.920, p < .0001). A significant difference in accuracy was observed across trial types (Fix_R vs. Fix_L vs. Conditional ($\chi^2(2)$ = 31.013, p < .0001). No significant difference in accuracy between fixed-left and fixed-right trials was observed (Z = -1.248, p = .212). Participants performed significantly better for both fixed-left (Z = -3.920, p < .001) and fixed-right (Z = -3.920, p < .001) compared to conditional trials.

Learning was quantified using a logistic regression algorithm designed to assess learning as a dynamic process across trials, creating representative curves which provide participants' probability of a correct response for any given trial (Smith & Brown, 2003; Smith et al., 2004). Learning onset was defined as the trial in which the lower-bound 95% confidence interval exceeded chance performance. There was a statistically significant difference in learning onset between the three trial types ($\chi^2(2)$ = 22.354, p < .001). Learning onset for fixed-left (median = 3.835, IQR = 2 - 7) and fixed-right (median = 3.833, IQR = 1 - 7) was not significantly different (Z = -0.081, p = .936). In contrast, learning onset was delayed for conditional (median = 11.5, IQR = 6 - 26) compared to fixed-left (Z = -3.267, p = .001) and fixed-right (Z = -3.435, p = .001) trials.

3.3.2 PROSPECTIVE PATTERN DISSIMILARITY OF HPC AND DAC INCREASES FROM EARLY TO LATE LEARNING

To assess how HPC and DAC contributions develop across prospective experience-based learning, I conducted a pattern dissimilarity analysis on first-level unsmoothed functional data for each of six experimental runs during periods preceding correct and incorrect conditional trials. I anatomically defined HPC and DAC bilaterally and calculated pattern dissimilarity between fixed trials immediately preceding correct and incorrect conditional trials (Figure 8A). I anticipated pattern dissimilarity preceding correct versus incorrect conditional trials would increase as learning progressed and greater pattern dissimilarity would be positively related to learning performance. Two analyses were conducted across image sets to test these predictions: (1) comparison of regional pattern dissimilarity for early and late learning, and (2) correlation analysis investigating the correlation between pattern dissimilarity and learning performance for early and late learning.

Confirming my first prediction, dissimilarity between patterns of activation was elevated for late, compared to early, task runs in both HPC ($t(19) = 4.42$, $p = 0.0003$) and DAC ($Z = 15.0$, $p = 0.0008$; Figure 8B, left). When comparing patterns of dissimilarity to overall performance across the sample, HPC exhibited a strong, positive relationship between pattern dissimilarity and performance during late learning ($r = 0.75$, $p = 0.001$) (Figure 8B, right) with a moderate, positive trend observed during early learning ($r = 0.44$, $p = 0.05$). In contrast, DAC demonstrated a strong, positive correlation between pattern dissimilarity and

performance for both late (r = 0.68, p = 0.0009) and early learning (r = 0.69, p = 0.0008).

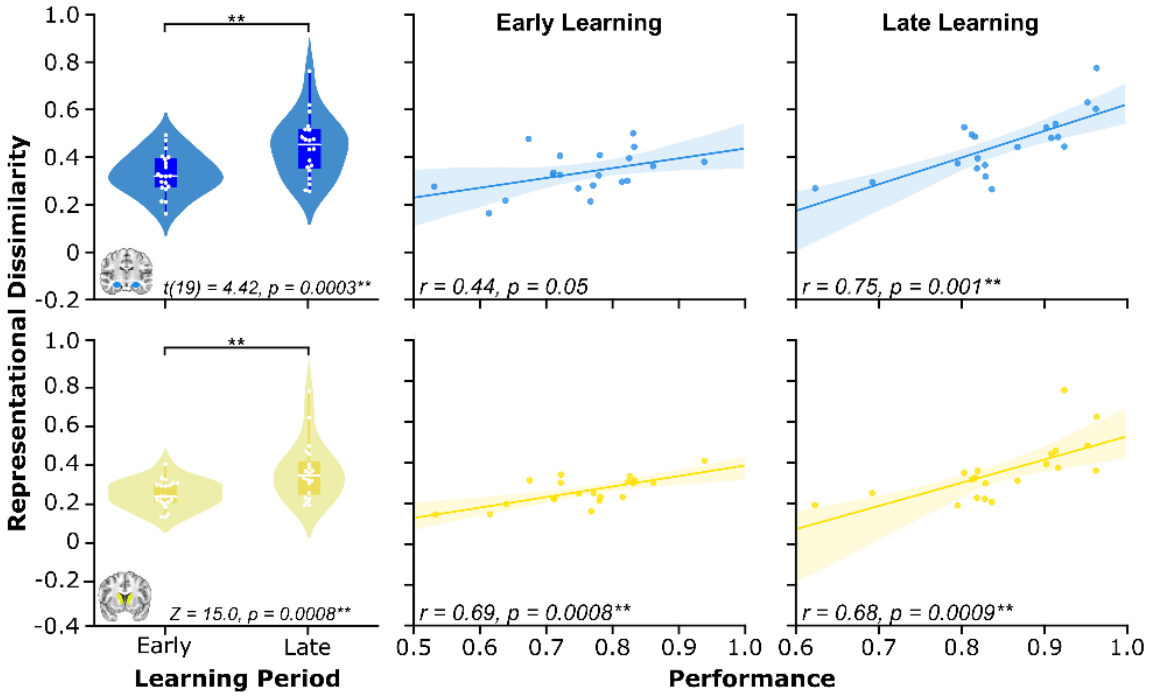

Figure 8. Pattern dissimilarity preceding correct and incorrect conditional trials for HPC and DAC increase from early to late learning. Anatomical ROIs include hippocampus (HPC) and dorsal anterior caudate (DAC). Violin plots with overlaid box and swarm plots represent 1-r correlation between region-specific activation pattern preceding correct and incorrect conditional trials (left). Greater representation dissimilarity was observed for HPC and DAC for late, compared to early, learning. Correlations between representational dissimilarity and participant performance (right) demonstrate while DAC dissimilarity is positively related to performance for both early and late learning, HPC dissimilarity is positively associated with performance only for late learning.

3.3.3 Concurrent DAC activation decreases as conditional task performance improves

To assess how HPC and DAC contributions develop across concurrent experience-based learning, I conducted a binned learning curve analysis on second-level functional data for each participant. The minimum and maximum

values of each participant's representative learning curve were used to create flexible boundaries for three discrete learning bins (Figure 9A): Bin 1 represented trials which fell into the lowest 1/3 of performance; Bin 2, the intermediate 1/3; and Bin 3, the highest 1/3 (Smith & Brown, 2003; Smith et al., 2004). A univariate model included regressors for activation during conditional trials which fell into Learning Bins 1, 2, and 3, as well as regressors of no interest. Anatomical bilateral ROIs were created for HPC and DAC, comparing second-level mean activation for conditional trials during each learning bin. I predicted an increased activation for both HPC and DAC during periods of high (Bin3), compared to those of either moderate (Bin 2) or low (Bin 1), performance. These predictions were informed by (1) my previous findings of DAC involvement in a concurrent network supporting choice execution, and (2) the abundance of evidence for the role of the HPC in retrieval processes (Gluth et al., 2015; Murty et al., 2016; Wimmer & Shohamy, 2012; Zeithamova, Dominick, et al., 2012; Zeithamova, Schlichting, et al., 2012; Zeithamova & Preston, 2010).

Interestingly, while a significant effect for learning bin was observed for DAC (Figure 9B; $F(2,38) = 4.09$, $p = 0.02$), the direction of this change was contrary to my predictions. Simple effects analysis revealed DAC activation for Bin 3 was significantly lower than Bin 1 ($t(19) = -3.39$, $p = 0.002$, $d = -0.64$), but was not significantly lower than Bin 2 ($t(19) = -0.70$, $p = 0.491$). A similar trend was observed for Bin 2 and Bin 1 ($t(19) = -1.91$, $p = 0.071$), through it did not reach significance. A trend for HPC in the predicted direction was observed (Figure 9B; $F(2,38) = 2.30$, $p = 0.11$), though it failed to reach significance.

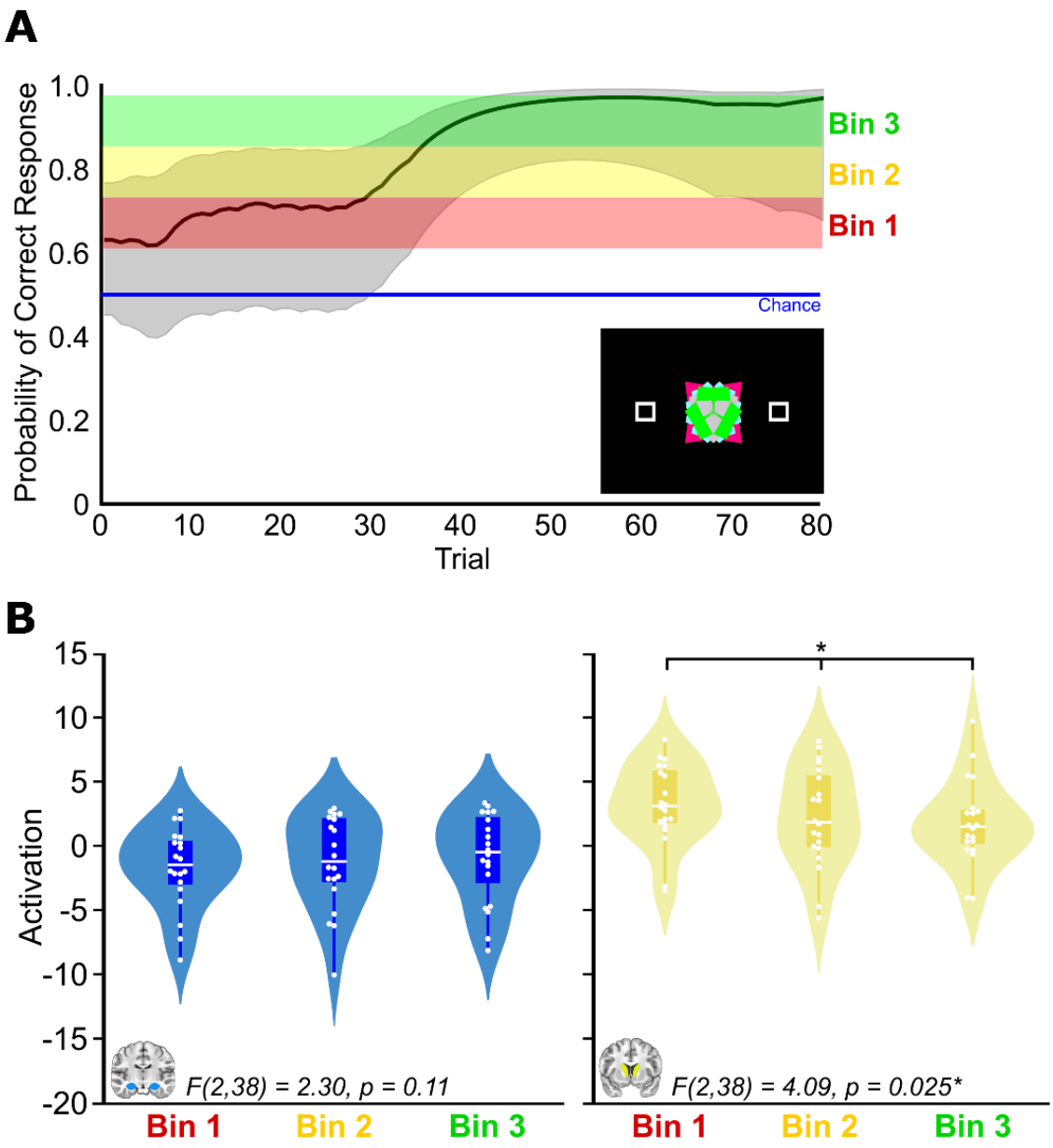

Figure 9. Decreased DAC activation during periods of high performance (A) Example learning curve demonstrating flexible binning of ROI activation for conditional trials based on probability of correct response. (B) Anatomical ROIs include hippocampus (HPC) and dorsal anterior caudate (DAC). Violin plots with overlaid box and swarm plots represent region-specific activation for each participant during performance tiers. A significant effect of learning bin was observed for DAC, with simple effects analysis revealing reduced activation of the DAC for high, compared to low, learning performance.

3.4 DISCUSSION

Most paradigms developed to investigate contributions of HPC to learning and memory focus on observations made during one of two temporal/process categories: (1) single instance of encoding novel information, or (2) retrieval during consistent performance, following extensive periods of learning. The current findings expand our understanding of how HPC and DAC support learning and the development of these mechanisms across time. In my pattern dissimilarity analysis, I demonstrate as learning develops from early to late stages in these regions, observed patterns of activation preceding correct and incorrect conditional behavior become increasingly dissimilar. Further, I provide evidence HPC and DAC pattern dissimilarity is positively related to learning performance. In other words, as these regional activation patterns preceding correct and incorrect performance become more distinct, conditional performance improves. For the DAC, this relationship is consistent across early and late learning; however, HPC exhibited a notable distinction between learning stage, demonstrating a significant dissimilarity-performance correlation only for late learning. In my binned learning analysis, I provide evidence the DAC exhibits decreased activation during periods of high, compared to low, performance.

My findings align with literature illustrating the indispensability of HPC to learning and memory processes. HPC engagement as a predictor to successful performance on memory-guided decision making tasks is well documented across human and animal studies (Hamm & Mattfeld, 2019; Jadhav et al., 2012; Palombo et al., 2015; Pfeiffer & Foster, 2013; Preston & Eichenbaum, 2013; Squire, 1992;

Squire et al., 2004; Stark et al., 2018). Beyond providing evidence for the involvement of HPC to learning and memory, my current design and subsequent results address a period and timescale of learning development often overlooked in the methodological midland between animal and human paradigms. In animal work, many experimental protocols necessitate extensive periods of task training to bring performance to criterion, investigating neurobiological processes during or immediately preceding decision behavior (Allen et al., 2014, 2016; Hadj-Bouziane et al., 2006; Histed et al., 2003; Jadhav et al., 2012; Jayachandran et al., 2019; Jones & Wilson, 2005b; Vertes, 2006; Yu & Frank, 2015). While yet other designs use high temporal resolution techniques to observe neural activity (e.g., single-cell recordings, local field potentials) as it occurs during encoding novel experience (Hadj-Bouziane & Boussaoud, 2003; Jadhav et al., 2016; Miyachi et al., 2002). On the other hand, human learning and memory paradigms often measure learning through performance following a single session encoding experience (Hamm & Mattfeld, 2019; Han et al., 2010; Jiang et al., 2015; Koch et al., 2008; Law et al., 2005; Mattfeld & Stark, 2011; Norman et al., 2019; Reeders et al., 2021; Zeithamova, Dominick, et al., 2012), or through comparison of task performance across repeated sessions over the course of days or weeks; in both cases, studies investigating human HPC correlates of learning have predominately focused on periods of retrieval.

Representational similarity analysis, or more specifically, pattern similarity/dissimilarity, offers a valid and reliable means to quantify unique patterns of neural activation in regions of interest during behaviorally-relevant epochs

across time (Xue et al., 2010). In three separate studies, Xue and associates (2010) demonstrated improved performance on tests of recognition and recall were associated with increased similarity of neural activation patterns across presentations during encoding. Here, I used pattern dissimilarity to explore how differences between neural activation patterns preceding successful and unsuccessful conditional performance changed across learning and how that change relates to conditional performance.

These findings provide evidence for dynamic contribution of the HPC across experience-based learning and demonstrate that unlike the DAC, for which differences in neural pattern activation was important to acquisition of conditional associations across both early and late learning, pattern dissimilarity was significantly related to performance only during late learning. These observations may reflect an improved stability of neural representations across learning as observed in Xue et al. (2010). Another possibility is development of improved late-learning retrieval resulting from increased practice. While the current methodological design is limited by an inability to determine with confidence which of these mechanistic changes is captured by my observations, these findings provide direction to future investigations exploring how neural representations influence learning development.

CHAPTER 4: PROSPECTIVE REPRESENTATIONAL CONTENT INFORMS SVM CLASSIFIER AS TO CORRECT CONDITIONAL TRIAL RESPONSE

4.1 INTRODUCTION

Aims 1 and 2 of my dissertation work investigated contributions of the HPC, mPFC, and striatum to prospective and concurrent memory-guided decision-making and how those contributions may evolve across learning. I observed the emergence of two distinct networks supporting memory-guided decision making: one whose contributions prospectively guided upcoming choice, and the second concurrent system which supported execution of correct decision-making behavior (Hamm & Mattfeld, 2019). Then in my learning analyses, I identified how contributions of the HPC and DAC change as performance improves and from early to late learning. For my final experiment, I sought to investigate possible neurobiological representations of prospective memory using multivoxel pattern analysis (MVPA).

MVPA is an analytic method which endeavors to identify highly reproducible patterns of voxel activation to differentiate between two or more experimental conditions (Chadwick et al., 2012; Mahmoudi et al., 2012; Weaverdyck et al., 2020). More specifically, decoding analyses are used to determine which condition gives rise to a specific pattern of activation. MVPA uses a supervised machine learning method known as a support vector machine (SVM) to perform either binary or multi-condition classification. While many univariate fMRI techniques are limited to magnitude of response from a particular region of interest, MVPA examines information contained within patterns of activation using “features”,

which are defined as select voxels (Weaverdyck et al., 2020). In this way, MPVA decoding (classification) analyses allow reversal of the direction of inference common to univariate fMRI techniques, allowing one to instead make determinations about experimental conditions given an observed pattern of voxel activation.

Machine learning classification has been successfully implemented with fMRI data to make inferences as to the nature and context of particular stimuli (Chadwick et al., 2012; Mahmoudi et al., 2012; van den Hurk et al., 2011; Weaverdyck et al., 2020). MVPA presumes if patterns of voxel activation can be used to predict stimulus membership within a particular class, then unique and identifiable information about that stimulus must be represented in the targeted region of interest. Such an ability makes MVPA a particularly useful tool to investigate the representational content of prospective memory-guided decision making.

To investigate the representational content of prospective memory-guided behavior, I designed a second visuomotor associative learning task similar to that used in Chapter 2 (Hamm & Mattfeld, 2019). However, this design doubled the number of possible conditional associations by including four fixed trials and one conditional trial. In this design, rather than associating a current conditional response (left or right) with the identity of a previous fixed-trial stimulus, participants learned through trial and error to associate previous stimulus-object fixed-trials with the current choice of either a face or a scene (Figure 10A). Previous findings had demonstrated not only were prospective mechanisms supporting

decision making (Chapter 2) but increases in prospective patterns of activation for the HPC and DAC were associated with improved performance (Chapter 3). Here, I investigated whether prospective voxel-based representational content could be identified in regions well-known for their representational clarity: fusiform face area (FFA) and parahippocampal place area (PPA). If a SVM classifier could be trained to categorize whether samples of prospective activation preceded either a face or scene conditional trial, such results would provide evidence of specific prospective representational content. Further, if such representational information can be demonstrated, the accuracy of the classifier when trained on these prospective sampled should be positively related to the performance of the participant.

With this complex multivariate approach, I investigated the possible informative nature of voxel-based representational content for prospective memory-guided decision making. While the SVM classifier accuracy was statistically better than would be expected by chance, no statistically significant relationships were observed between classifier and participant conditional performance.

4.2 METHODS

Thirty-three right-handed volunteers (13 female, mean age = 25.53, SD = 5.78) at Florida International University were recruited to perform a conditional visuo-motor association learning task in a magnetic resonance imaging scanner. All participants provided written informed consent in accordance with local Institutional Review Board requirements. Individuals were recruited from the Florida International University community and financially compensated for their

time. Eight individuals were excluded from the reported analyses. Six were removed because of technical difficulties resulting from programming error in the task software. One participant was removed after reporting use of antidepressants following data collection. Lastly, one participant was removed due to significant incidental findings. The final sample size was 25 participants (13 females; mean age = 25.21 years, SD = 5.00).

4.2.1 BEHAVIORAL PROCEDURES

4.2.1.1 FUNCTIONAL LOCALIZATION TASK (LOC)

Participants completed two runs of a block-design "functional localization" task requiring "yes/no" judgments on three categories of visual stimuli. Images were presented, one per trial, in separate blocks consisting of faces, scenes, and numbers. Face and scene blocks each contained 20 trials in which participants indicated whether the current (1) face was female or (2) scene contained water. Number blocks contained 10 trials each in which participants indicated whether the current number was less or greater than five. Responses were recorded using a MR-compatible response box. For face and scene trials, a left response on the response box indicated "Yes" and right indicated "No". For number trials, a left response indicated "less than", while right indicated "greater than". Each trial lasted for 1250 ms. Blocks sequence was face-number-scene-number, repeated seven times, for a total of 140 presentations of each stimulus-type per run. Participants completed two functional localization runs (280 per type, 840 trials in total).

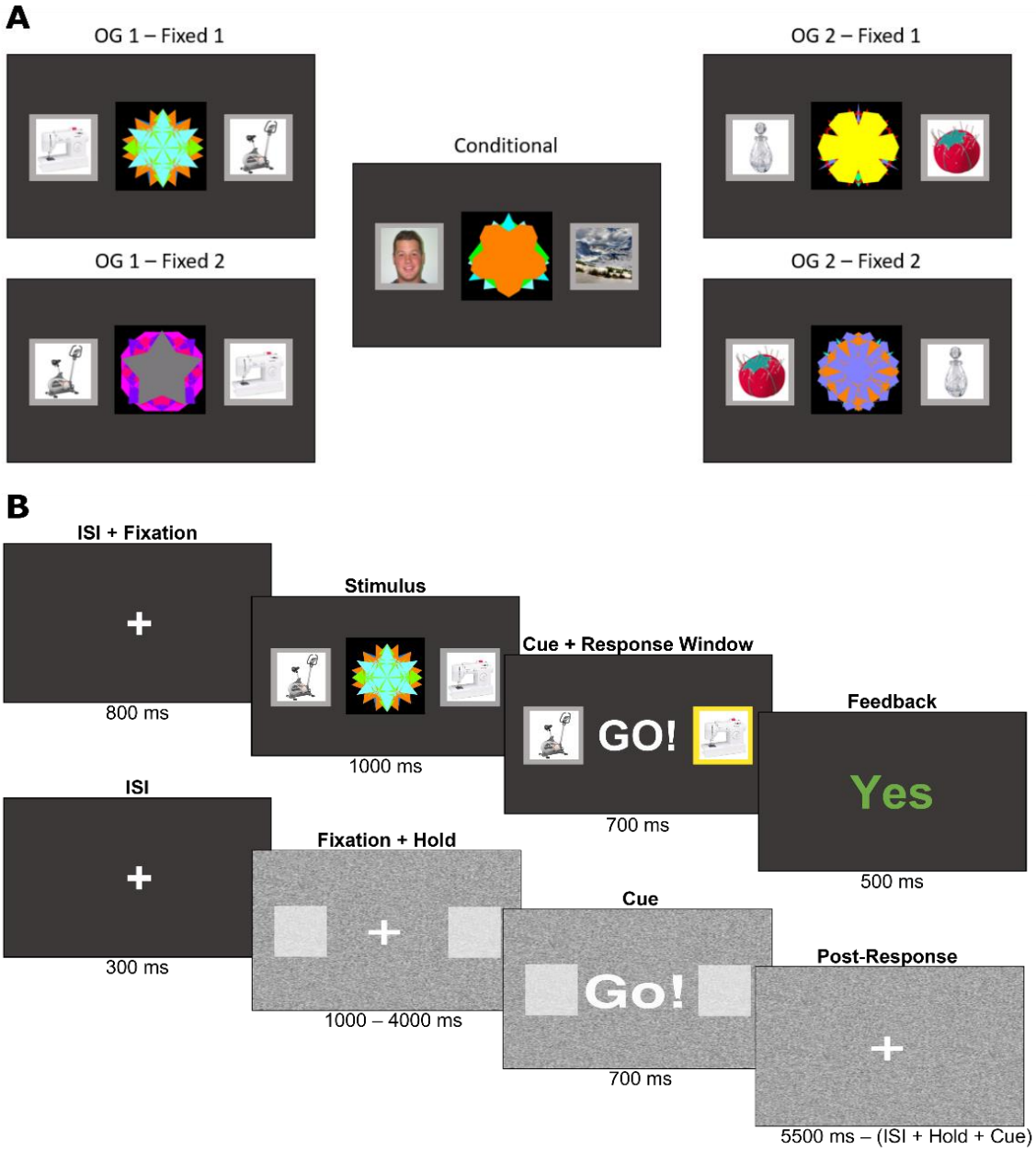

Figure 10. Schematic diagram of vCAT2 associations and object groups. (A) Five kaleidoscopic association trials, four fixed object-associations, and one conditional face/scene-association. Fixed trials are split into two object groups (*OG*). Yellow boxes indicate the correct association for each trial. One fixed stimulus-object association from each OG is associated with a correct conditional response of "face", while the other stimulus-object association from each OG is associated with "scene". (B) Task and BL trials were similar in structure but not timing. Total BL trial duration was 5500 ms, with variable fixation+hold and post-response periods.

4.2.1.2 CONDITIONAL ASSOCIATIVE TASK #2 (VCAT2)

The task was modified from the visuo-motor conditional associative learning task used in Chapter 2 (Hamm & Mattfeld, 2019; Law et al., 2005; Mattfeld & Stark, 2011; Stark et al., 2018). For each task trial, participants associated a visual stimulus with one of two possible choices (Figure 9). Stimuli consisted of five computer-generated kaleidoscopic images, presented one at a time, and centered between two gray squares containing images of either objects (fixed trials), or face and scene (conditional trials). Participants were asked to determine, through trial and error, the relationship between each kaleidoscopic image and one of the two flanking images. Responses were registered by pressing with either an index (*Button 1 - indicating left box*) or middle finger (*Button 2 - indicating right box)* using an MR-compatible response box. Three types of trials were presented:

(1) Stimulus-object association (*fixed*) trials. For these trials, participants were asked to learn the association between common, everyday objects and four kaleidoscopic images. There were four possible choice objects, grouped into two object groups – meaning two objects were always presented together as choice options for two of the kaleidoscopic stimulus trials (Object Groups or OG; Figure 9A). Within each of these object groups, one fixed stimulus-object association trial would come to be associated with a face (Fixed 1, Figure 9B), while the other would be associated with a scene, on subsequent conditional association trials (Fixed 2, Figure 9C). Correct associations for these four stimulus-object trials were “fixed” and remained consistent across all presentations; however, object position (left or right) relative to stimulus and its

respective response were not static across presentations. Correct screen-location response changed per trial depending on which side the associated object was presented.

(2) Preceding stimulus-object to current face/scene association (*conditional*) trials. For the fifth kaleidoscopic image, participants were tasked with determining a more temporally complex association between the correct preceding stimulus-object response and either face or scene (Conditional, Figure 9A-C). One stimulus-object association from each of the two object groups would be correctly associated with face (Figure 9B) while the other from each group would be associated with scene (Figure 9C). Similar to fixed trials, correct response was dependent on which side of the screen face and scene were presented.

(3) Baseline trials (*BL*). During these trials, participants were asked to select the "whiter" of two boxes. BL trials were similar to learning trials in sequence but not timing, lasting 5500 ms per BL trial. Duration of fixation+hold and post-response phases varied across presentations. Due to decreased cognitive load in responding to these trials, BL followed fixed trials to provide both an extended duration of prospective activation, as well as a longer temporal window to accommodate the hemodynamic response for use in multivoxel pattern analysis.

Learning trials (*fixed* and *conditional*; 3000 ms total duration each) consisted of three sequential phases: (1) fixation, (2) stimulus presentation and response, and (3) feedback. Each of the four fixed stimulus-object association trial

was presented 100 times across four experimental runs (25 per run). Conditional association trials were presented 200 times across four experimental runs (50 per run) and could only follow a fixed association in trial sequence. Finally, BL trials were presented 120 times across four experimental runs (30 per run) and like conditional trials, could only follow a fixed association in trial sequence.

As previously defined in the vCAT1 experiment in Chapter 2, perceptual baseline trials were comprised of a random static image created through binarization of random values for each pixel of screen resolution (1280 x 800). Randomly generated pixel values greater than 0.85 became white, while those below threshold became gray. A white fixation cross between two white outlined boxes was presented at the center of the screen over the static background. In identical fashion to the underlying static image, contents of each box were also random patterns (320 x 200); however, the binarization threshold to produce a white pixel was considerably lower and, for target, vacillated as a function of performance. For the first BL trial, binarization thresholds for target and foil were initially set at 0.55 and 0.65, respectively. Participants were asked to identify which of the two boxes was “whiter”. If the participant responded correctly to seven out of the previous 10 trials, the white threshold for target box would increase by 10% of last trial, producing fewer white pixels and bringing the image closer to the constant foil threshold of 0.65, thereby increasing difficulty. Conversely, if response to fewer than five of the preceding 10 BL trials were correct, threshold decreased by 10% of previous trial value, resulting in a “whiter” target and easier identification.

Each BL trial lasted for a duration of 5500 ms and could only follow fixed trials in presentation sequence.

4.2.2 PRESCAN TRAINING

All participants received training of 180 total trials (150 learning stimuli and 30 BL trials) using a practice set of five images (four fixed, one conditional) specific to the training session. Training allowed participants to become acquainted with task nature and timing to mitigate loss of trials due to nonresponse at the beginning of the first experimental run. Training was conducted on a MacBook Pro using identical finger-response mapping as scanning session.

4.2.3 MRI METHODS

Imaging data were acquired on a Siemens Magnetom Prisma 3T scanner with a 32-channel head coil at the Center for Imaging Science at Florida International University (Miami, FL). Functional images were obtained using a T2*-sensitive gradient echo pulse sequence (66 interleaved axial slices, a slice thickness = 2.0 mm, TR = 1760 ms, TE = 35 ms, flip angle = 52˚, FOV = 200 mm, voxel size = 2.0 x 2.0 x 2.0 mm^3). Three hundred and four whole-brain images were collected for each run of the functional localization task (LOC). Three hundred and fifty-six whole-brain images were collected per run for advanced visuomotor conditional association task (vCAT2). For purposes of coregistration and registration, high-resolution three-dimensional magnetization-prepared rapid gradient echo sequence collected (MP-RAGE: 176 axial slices, slice thickness = 1.0 mm, TR = 2500 ms, TE = 2.9 ms, flip angle = 8˚, voxel FOV = 256 mm, size = 1.0 x 1.0 x 1.0 mm^3). Data were preprocessed and analyzed

using the following software packages: Analysis of Functional Neuroimages (AFNI version 16.3.18; Cox, 1996), FMRIB Software Library (FSL version 5.0.8; Jenkinson et al., 2012), FreeSurfer (FS version 6.0.0; Fischl, 2012), Advanced Normalization Tools (ANTs version 2.1.0; Avants et al., 2008), and Neuroimaging in Python (Nipype version 1.0.0.dev0; Gorgolewski, 2016) pipeline. T1-weighted structural scans underwent cortical surface reconstruction and cortical/subcortical segmentation. Surface reconstruction was visually inspected and errors were manually edited and resubmitted. Functional data were first 'despiked', removing and replacing intensity outliers in the functional time series. Simultaneous slice timing and motion correction (Roche, 2011) was performed, aligning all functional volumes to the middle volume of the first run. An affine transformation was calculated to co-register functional data to their structural scan. Motion and intensity outlier timepoints (>1 mm frame-wise-displacement; >3 SD mean intensity) were identified. Functional data were spatially filtered with a 5 mm kernel using *SUSAN* algorithm (FSL; Smith & Brady, 1997), which preserves the underlying structure by only averaging local voxels with similar intensities.

Anatomical images were skull-stripped and then registered to MNI-152 template via a rigid body transformation (FSL FLIRT; DOF = 6). This step was used to minimize large differences in position across participants and generate a template close to a commonly used reference. ANTs (Avants et al., 2008) software was used to create a study-specific template to minimize normalization error for any given participant. Each participant's skull-stripped brain was normalized using non-linear symmetric diffeomorphic mapping implemented by ANTS. The resulting

warps were applied to contrast parameter estimates following fixed-effects modeling for subsequent group-level tests.

4.2.4 ANATOMICAL REGIONS OF INTEREST

Two anatomical regions of interest (ROIs) were bilaterally defined using each participant's structural scan. The fusiform face area (FFA) and parahippocampal place area (PPA) were defined by binarizing segmentations from FreeSurfer aparc+aseg.mgz files. All masks were back-projected to functional space for analysis.

4.2.5 MULTIVOXEL PATTERN ANALYSIS – FUNCTIONAL LOCALIZER

fMRI data collected during the functional localization task were analyzed using FSL based on principles of the general linear model. A single univariate, block-design model was used to create unsmoothed, functional masks isolating voxel-wise activation for faces and scenes. All models included regressors of no interest which consisted of motion parameters (x, y, z translations; pitch, roll, yaw rotations), first and second derivatives of the motion parameters, normalized motion, first, second, and third order Lagrange polynomials, as well as each outlier time-point that exceeded artifact detection thresholds. The regressors of interest consisted of face, scene, and number trial blocks. Contrasts examined differences in activation between face and scene blocks, as well as face and number blocks and scene and number blocks. Event regressors were convolved with FSL's double gamma hemodynamic response function with an onset coinciding with stimulus presentation and a duration of 3 seconds. Following first-level analyses, fixed-effects analyses across experimental runs were performed for each

participant for each respective contrasts of interest. The product of anatomical ROI masks and standardized, unsmoothed second-level copes for faces > scenes and scenes > faces contrasts from the LOC task with a minimum intensity threshold of 3.2775 were obtained, producing a template constrained by both region and activation for isolating features.

4.2.6 MULTIVOXEL PATTERN ANALYSIS – VCAT2

A least-squares separate (LS-S) approach (Mumford et al., 2012) was used for analysis of functional data from the visuomotor conditional association task. The LS-S method runs a separate GLM for each trial of interest, collapsing all other similar trials into a single nuisance regressor. The LS-S approach has been demonstrated as the most accurate approach for estimating trial-by-trial signals in event-related designs, and thus providing optimal trial samples for training and testing with the SVM classifier. Trials of interest were defined as sequential fixed-BL trial pairs (fixed 3000 ms, BL 5500ms, total 8500 ms). A separate general linear model was run for each trial pair of interest. All first-level models included a regressor for single relevant trial pair and all remaining task and nuisance regressors with relevant trials were removed from its respective task regressor. *A priori* anatomical regions of interest were defined as in previous chapters and binarized ROI masks were created.

4.2.7 CLASSIFIER TRAINING

The MVPA decoding analysis utilized a SVM to perform classification after training to identify potential relationships between patterns of voxel activation in the fusiform face area (FFA) and parahippocampal place area (PPA), and whether

the anticipated correct response for subsequent conditional trials would be either a face or scene. To achieve this, I provided a support vector classifier (SVC) with “features” consisting of voxels in the FFA and PPA which demonstrated selective activation when presented with either faces or scenes during the functional localizer task (LOC). This effort to isolate functionally selective voxels within larger anatomical regions was performed to reduce the overall number of features, thereby increasing samples-to-features ratio, minimizing possible noise, and improving classifier performance. The “samples” given to the classifier were individual fixed trials preceding either conditional or baseline trials, along with labels indicating whether the fixed stimulus-object trials would be associated with a face or scene on subsequent conditional trials.

Due to the simplicity of only two possible conditions (face or scene), I selected a simple linear support vector classifier by Scikit-learn (LinearSVC; Pedregosa et al., 2011). For classifier training, I used a leave-one-sample-out method in which there were approximately 320 individual SVC models per participant. In other words, the classifier iterated through each provided sample, trained on the remaining 319, and tested on the single, current sample. The outputs of these individual models provided 320 binary scores representing classifier performance for each test sample (0 incorrect, 1 correct). These binary performance values were then averaged to produce an overall metric of classifier accuracy. In addition to raw accuracy, individual binary outputs of each model were used to first calculate the precision and recall of the classifier, and ultimately the harmonic mean (F1-score):

$$Precision = \frac{True\ Positives}{True\ Positives + False\ Positives}$$

$$Recall = \frac{True\ Positives}{True\ Positives + False\ Negatives}$$

$$F1\ Score\ (Harmonic\ mean) = 2\frac{Precison \times Recall}{Precision + Recall}$$

4.3 RESULTS

4.3.1 BEHAVIORAL PERFORMANCE

Participants were more accurate on fixed compared to conditional trials, with no differences in reaction time, and both were performed better than chance. For distributions that violated assumptions of parametric methods (i.e., accuracy and onset of learning), non-parametric Wilcoxon Signed-Rank and Spearman's correlation coefficient tests were performed. All results were Bonferroni corrected for multiple comparisons where appropriate. To determine whether participants performed better than chance, median accuracy was calculated across stimulus sets for each participant. Participants demonstrated significantly better than chance performance for fixed (Fixed: mean = 0.92, SD = 0.05; Fixed vs chance: $t(24) = 41.14$, $p < 0.0001$) and conditional images (Conditional: median = 0.84, IQR = 0.07; Conditional vs. chance: $Z = 4.0$, $p < 0.0001$) trials. When comparing performance between trial types (Fixed vs. Conditional), a significant difference for

accuracy was observed ($Z = 1.0$, $p < 0.0001$). No statistically significant difference was observed for response time between fixed (mean = 0.268, SD = 0.047) and conditional (mean = 0.27, SD = 0.04) trials ($t(24) = -0.31$, $p = 0.75$) trials.

4.3.2 MULTIVOXEL PATTERN ANALYSIS

An LSS modeling approach was implemented in which each trial of interest was modeled separately. This technique was used in conjunction with features selected via the intersection of anatomical masks (FFA and PPA) and voxel activation responsiveness to specific stimuli (face and scene). When looking at accuracy (mean = 0.54, SD = 0.05), the SVC performed statistically better than chance ($t(24) = 3.96$, $p = 0.002$). Additionally, when the F1 score is calculated (mean = 0.53, SD = 0.05), the SVC performance is better than chance performance as well ($t(24) = 2.29$, $p = 0.007$). No statistically significant difference was observed between SVC performance in predicting faces (mean = 0.53, SD = 0.07) and scenes (mean = 0.52, SD = 0.09). With regard to a possible relationship between classifier and participant performance, no statistical evidence was found ($r_S = 0.12$, $p = 0.55$).

4.4 DISCUSSION

In this experiment, I investigated representational content of prospective memory-guided behavior using a machine learning algorithm known as a support vector classifier (SVC). While classifier and participant performance did not demonstrate a significant correlation, when observing accuracy, the classifier was able to perform significantly better than would be expected by chance. However, calculation of the F1 score considers both precision (positive predictive value) and

recall (sensitivity), making it a more robust metric for use with datasets containing possible imbalances (uneven number of samples per condition) and use of random cross-validation techniques (such as leave-one-sample-out) for training-testing (Mahmoudi et al., 2012; Weaverdyck et al., 2020). Even when using this more conservative metric, the classifier's performance, compared to chance, was still significant, $t(24) = 2.29$, $p = 0.007$.

These results are harmonious with a previous study using a similar methodological design (Doll et al., 2015) in which prospective activations were identified in functionally-localized regions of interest during a complex reward-learning task. While Doll et al. (2015) selected regions of the visual pathway, in the current design I have investigated possible prospective activations preceding conditional associative decision making in FFA (Contreras et al., 2013; van den Hurk et al., 2011; Zhang et al., 2015) and PPA (Diana et al., 2008; M. Johnson & Johnson, 2014, 2014; Park & Park, 2015; Sun et al., 2021), two regions well-known for their responsiveness to faces and scenes, respectively. Using functionally-select features from these regions, each region-specific SVC was able to perform better than chance in determining whether observed patterns of activations would precede a correct face or scene response on subsequent conditional trials. The ability of the classifiers to perform better than chance suggests identifiable patterns of activation in these regions may indeed carry information about representational content which can be used to inform prospective memory-guided behavior.

A limitation to consider with the use of MVPA classifier sensitivity to the balance between features and samples. Generally speaking, the number of

samples should be maximized and features minimized to improve samples-to-features ratio, in order to reduce noise in smaller-sample studies (Weaverdyck et al., 2020). The current design, as with most fMRI task designs, could benefit from a greater number of target trials to improve power and the sample-to-features ratio.

Future directions should include investigations into possible representational content contained within regions known for their contributions to both prospective and concurrent memory-guided behavior. The HPC, striatum, and mPFC may contain unique and identifiable patterns of prospective voxel activations related to faces, scenes, or other decodable stimulus features. The prospective FFA/PPA activations observed here may well be linked to similar engagement of the HPC for scene-related stimuli, as these regions have demonstrated unique increased coactivation when presented with novel scene images during episodic memory tasks. (Köhler et al., 2002). Similarly, HPC and FFA coactivation occurs when participants are presented with novel, but not repeated, faces (Liu et al., 2017) or face-object associations (Schlichting & Preston, 2016).

CONCLUSION

In order to make successful decisions, it is often necessary to call upon past events to inform our behavior. The commonsense notion that one's past predicts his or her future does little justice to the intricacy of neurobiological mechanisms supporting memory-guided decision making. In Chapter 2, I provided evidence of prospective and concurrent memory-guided networks of cortical and subcortical regions which included the HPC and DAC, respectively. In the prospective network, the HPC, mPFC, PUT, and other cortical structures exhibited enhanced activation preceding successful conditional decisions. The second network consisted of the DAC, dlPFC, and other cortical regions which demonstrated increased activation during execution of successful decision making. However, an important limitation of those analytic designs was the unanswered question of how contributions of these networks might evolve with experience.

In Chapter 3, my approach to assessing learning-induced changes to these prospective and concurrent circuits used two analytic methods: (1) patten dissimilarity analysis and (2) a binned learning curve technique. I observed increased pattern dissimilarity of the HPC and DAC for periods proceeding correct, compared to incorrect, conditional trial performance from early to late learning. Simply put, prospective patterns of voxel activation in these two regions for correct and incorrect performance became more dissimilar from early to late learning. Further, while DAC pattern dissimilarity facilitated learning during both early and late learning, HPC pattern dissimilarity only demonstrated such a relationship with performance for late learning. This finding provides fascinating new evidence for

the dynamic and evolving nature of HPC engagement across experience-based learning. Additionally, the binned learning analysis of mean regional activation during conditional trials provided evidence that as learning performance improves, DAC involvement wanes. Conversely, a slight trend was observed for HPC of increased activation from periods of low to high performance.

The significant results of the pattern dissimilarity learning analysis hinted toward the possibility of potential prospective representational content being contained within these patterns of region-specific, voxel activation. In order to address this possibility, a second task was created for the express purpose of conducting MVPA. I trained an SVC to perform binary categorization of target trial samples using features selected via the intersection of anatomical and functionally localized masks. The SVC performed better than would be expected by chance, indicating voxel activation within the features contained some degree of representational information which supported classifier performance.

Taken together, these findings within my dissertation work provide new evidence for distinct temporal and mechanistic contributions of the HPC, striatum, and mPFC which facilitate memory-guided decision making through both prospective and concurrent neurobiological processes.

REFERENCES

Addis, D. R., Wong, A. T., & Schacter, D. L. (2007). Remembering the past and imagining the future: Common and distinct neural substrates during event construction and elaboration. *Neuropsychologia*, *45*(7), 1363–1377. https://doi.org/10.1016/j.neuropsychologia.2006.10.016

Allen, T. A., Morris, A. M., Mattfeld, A. T., Stark, C. E., & Fortin, N. J. (2014). A sequence of events model of episodic memory shows parallels in rats and humans: Sequence Memory In Rats And Humans. *Hippocampus*, *24*(10), 1178–1188. https://doi.org/10.1002/hipo.22301

Allen, T. A., Morris, A. M., Stark, S. M., Fortin, N. J., & Stark, C. E. (2015). Memory for sequences of events impaired in typical aging. *Learning & Memory*, *22*(3), 138–148. https://doi.org/10.1101/lm.036301.114

Allen, T. A., Salz, D. M., McKenzie, S., & Fortin, N. J. (2016). Nonspatial sequence coding in CA1 neurons. *Journal of Neuroscience*, *36*(5), 1547–1563.

Avants, B. B., Epstein, C. L., Grossman, M., & Gee, J. C. (2008). Symmetric diffeomorphic image registration with cross-correlation: Evaluating automated labeling of elderly and neurodegenerative brain. *Medical Image Analysis*, 16.

Balleine, B. W., Delgado, M. R., & Hikosaka, O. (2007). The role of the dorsal striatum in reward and decision-making. *Journal of Neuroscience*, *27*(31), 8161–8165. https://doi.org/10.1523/JNEUROSCI.1554-07.2007

Barbas, H., & Blatt, G. J. (1995). Topographically specific hippocampal projections target functionally distinct prefrontal areas in the rhesus monkey. *Hippocampus*, *5*(6), 511–533. https://doi.org/10.1002/hipo.450050604

Beck, S. M., Ruge, H., Walser, M., & Goschke, T. (2014). The functional neuroanatomy of spontaneous retrieval and strategic monitoring of delayed intentions. *Neuropsychologia*, *52*, 37–50. https://doi.org/10.1016/j.neuropsychologia.2013.10.020

Benchenane, K., Peyrache, A., Khamassi, M., Tierney, P. L., Gioanni, Y., Battaglia, F. P., & Wiener, S. I. (2010). Coherent theta oscillations and reorganization of spike timing in the hippocampal-prefrontal network upon learning. *Neuron*, *66*(6), 921–936. https://doi.org/10.1016/j.neuron.2010.05.013

Benoit, R. G., Gilbert, S. J., Frith, C. D., & Burgess, P. W. (2012). Rostral prefrontal cortex and the focus of attention in prospective memory. *Cerebral Cortex*, *22*(8), 1876–1886. https://doi.org/10.1093/cercor/bhr264

Blazquez, P. M., Fujii, N., Kojima, J., & Graybiel, A. M. (2002). A network representation of response probability in the striatum. *Neuron*, *33*(6), 973–982. https://doi.org/10.1016/S0896-6273(02)00627-X

Bonnici, H. M., Chadwick, M. J., Lutti, A., Hassabis, D., Weiskopf, N., & Maguire, E. A. (2012). Detecting representations of recent and remote autobiographical memories in vmPFC and hippocampus. *Journal of Neuroscience*, *32*(47), 16982–16991. https://doi.org/10.1523/JNEUROSCI.2475-12.2012

Bornstein, A. M., & Daw, N. D. (2012). Dissociating hippocampal and striatal contributions to sequential prediction learning: Sequential predictions in hippocampus and striatum. *European Journal of Neuroscience*, *35*(7), 1011–1023. https://doi.org/10.1111/j.1460-9568.2011.07920.x

Bornstein, A. M., Khaw, M. W., Shohamy, D., & Daw, N. D. (2017). Reminders of past choices bias decisions for reward in humans. *Nature Communications*, *8*(1), 15958. https://doi.org/10.1038/ncomms15958

Brandimonte, M., Einstein, G. O., & McDaniel, M. A. (1996). *Prospective Memory: Theory and Applications*.

Brasted, P. J., & Wise, S. P. (2004). Comparison of learning-related neuronal activity in the dorsal premotor cortex and striatum. *European Journal of Neuroscience*, *19*(3), 721–740. https://doi.org/10.1111/j.0953-816X.2003.03181.x

Braver, T. S. (2012). The variable nature of cognitive control: A dual mechanisms framework. *Trends in Cognitive Sciences*, *16*(2), 106–113. https://doi.org/10.1016/j.tics.2011.12.010

Brincat, S. L., & Miller, E. K. (2015). Frequency-specific hippocampal-prefrontal interactions during associative learning. *Nature Neuroscience*, *18*(4), 576–581. https://doi.org/10.1038/nn.3954

Brovelli, A., Nazarian, B., Meunier, M., & Boussaoud, D. (2011). Differential roles of caudate nucleus and putamen during instrumental learning. *NeuroImage*, *57*(4), 1580–1590. https://doi.org/10.1016/j.neuroimage.2011.05.059

Burgess, P. W., Gonen-Yaacovi, G., & Volle, E. (2011). Functional neuroimaging studies of prospective memory: What have we learnt so far? *Neuropsychologia*, *49*(8), 2246–2257. https://doi.org/10.1016/j.neuropsychologia.2011.02.014

Burgess, P. W., Scott, S. K., & Frith, C. D. (2003). The role of the rostral frontal cortex (area 10) in prospective memory: A lateral versus medial

dissociation. *Neuropsychologia*, *41*(8), 906–918. https://doi.org/10.1016/S0028-3932(02)00327-5

Carr, M. F., Jadhav, S. P., & Frank, L. M. (2011). Hippocampal replay in the awake state: A potential physiological substrate of memory consolidation and retrieval. *Nature Neuroscience*, *14*(2), 147–153.

Cavaco, S., Anderson, S. W., Correia, M., Magalhães, M., Pereira, C., Tuna, A., Taipa, R., Pinto, P., Pinto, C., Cruz, R., Lima, A. B., Castro-Caldas, A., da Silva, A. M., & Damásio, H. (2011). Task-specific contribution of the human striatum to perceptual–motor skill learning. *Journal of Clinical and Experimental Neuropsychology*, *33*(1), 51–62. https://doi.org/10.1080/13803395.2010.493144

Cavada, C. (2000). The Anatomical Connections of the Macaque Monkey Orbitofrontal Cortex. A Review. *Cerebral Cortex*, *10*(3), 220–242. https://doi.org/10.1093/cercor/10.3.220

Chadwick, M. J., Bonnici, H. M., & Maguire, E. A. (2012). Decoding information in the human hippocampus: A user's guide. *Neuropsychologia*, *50*(13), 3107–3121. https://doi.org/10.1016/j.neuropsychologia.2012.07.007

Cohen, J. D., & O'Reilly, R. C. (1996). A preliminary theory of the interactions between prefrontal cortex and hippocampus that contribute to planning and prospective memory. In *Prospective Memory: Theory and Applications* (pp. 267–296). Lawrence Erlbaum Associates.

Cona, G., Kliegel, M., & Bisiacchi, P. S. (2015). Differential effects of emotional cues on components of prospective memory: An ERP study. *Frontiers in Human Neuroscience*, *9*. https://doi.org/10.3389/fnhum.2015.00010

Contreras, J. M., Banaji, M. R., & Mitchell, J. P. (2013). Multivoxel Patterns in Fusiform Face Area Differentiate Faces by Sex and Race. *PLOS ONE*, *8*(7), e69684. https://doi.org/10.1371/journal.pone.0069684

Cooper, J. C., Dunne, S., Furey, T., & O'Doherty, J. P. (2012). Human Dorsal Striatum Encodes Prediction Errors during Observational Learning of Instrumental Actions. *Journal of Cognitive Neuroscience*, *24*(1), 106–118. https://doi.org/10.1162/jocn_a_00114

Cox, R. W. (1996). AFNI: Software for analysis and visualization of functional magnetic resonance neuroimages. *Computers and Biomedical Research*, *29*(3), 162–173. https://doi.org/10.1006/cbmr.1996.0014

de la Vega, A., Chang, L. J., Banich, M. T., Wager, T. D., & Yarkoni, T. (2016). Large-scale meta-analysis of human medial frontal cortex reveals tripartite

functional organization. *The Journal of Neuroscience*, *36*(24), 6553–6562. https://doi.org/10.1523/JNEUROSCI.4402-15.2016

Diana, R. A., Yonelinas, A. P., & Ranganath, C. (2008). High-resolution multi-voxel pattern analysis of category selectivity in the medial temporal lobes. *Hippocampus*, *18*(6), 536–541. https://doi.org/10.1002/hipo.20433

Diba, K., & Buzsáki, G. (2007). Forward and reverse hippocampal place-cell sequences during ripples. *Nature Neuroscience*, *10*(10), 1241–1242.

Dickinson, A., & Balleine, B. (1994). Motivational control of goal-directed action. *Animal Learning & Behavior*, *22*(1), 1–18. https://doi.org/10.3758/BF03199951

Doll, B. B., Duncan, K. D., Simon, D. A., Shohamy, D., & Daw, N. D. (2015). Model-based choices involve prospective neural activity. *Nature Neuroscience*, *18*(5), 767–772. https://doi.org/10.1038/nn.3981

Ego-Stengel, V., & Wilson, M. A. (2010). Disruption of ripple-associated hippocampal activity during rest impairs spatial learning in the rat. *Hippocampus*, *20*, 1–10.

Eichenbaum, H., & Cohen, N. J. (1988). Representation in the hippocampus: What do hippocampal neurons code? *Trends in Neurosciences*, *11*(6), 244–248. https://doi.org/10.1016/0166-2236(88)90100-2

Einstein, G. O., & McDaniel, M. A. (2005). Prospective Memory: Multiple Retrieval Processes. *Current Directions in Psychological Science*, *14*(6), 286–290. https://doi.org/10.1111/j.0963-7214.2005.00382.x

Ellis, J. (1996). In *Prospect Memory: Theories and Applications*. Lawrence Erlbaum Associates.

Euston, D. R., Gruber, A. J., & McNaughton, B. L. (2012). The role of medial prefrontal cortex in memory and decision making. *Neuron*, *76*(6), 1057–1070. https://doi.org/10.1016/j.neuron.2012.12.002

Ferbinteanu, J., & Shapiro, M. L. (2003). Prospective and Retrospective Memory Coding in the Hippocampus. *Neuron*, *40*(6), 1227–1239. https://doi.org/10.1016/S0896-6273(03)00752-9

Fischl, B. (2012). FreeSurfer. *NeuroImage*, *62*(2), 774–781. https://doi.org/10.1016/j.neuroimage.2012.01.021

Flaherty, A., & Graybiel, A. (1994). Input-output organization of the sensorimotor striatum in the squirrel monkey. *The Journal of Neuroscience*, *14*(2), 599–610. https://doi.org/10.1523/JNEUROSCI.14-02-00599.1994

Fonov, V., Evans, A. C., Botteron, K., Almli, C. R., McKinstry, R. C., & Collins, D. L. (2011). Unbiased average age-appropriate atlases for pediatric studies. *NeuroImage*, *54*(1), 313–327. https://doi.org/10.1016/j.neuroimage.2010.07.033

Fonov, V., Evans, A., McKinstry, R., Almli, C., & Collins, D. (2009). Unbiased nonlinear average age-appropriate brain templates from birth to adulthood. *NeuroImage*, *47*, S102. https://doi.org/10.1016/S1053-8119(09)70884-5

Foster, D. J., & Wilson, M. A. (2006). Reverse replay of behavioural sequences in hippocampal place cells during the awake state. *Nature*, *440*(7084), 680–683. https://doi.org/10.1038/nature04587

François-Brosseau, F.-E., Martinu, K., Strafella, A. P., Petrides, M., Simard, F., & Monchi, O. (2009). Basal ganglia and frontal involvement in self-generated and externally-triggered finger movements in the dominant and non-dominant hand. *European Journal of Neuroscience*, *29*(6), 1277–1286. https://doi.org/10.1111/j.1460-9568.2009.06671.x

Frank, L. M., Brown, E. N., & Wilson, M. (2000). Trajectory Encoding in the Hippocampus and Entorhinal Cortex. *Neuron*, *27*(1), 169–178. https://doi.org/10.1016/S0896-6273(00)00018-0

Gilbert, S. J. (2011). Decoding the content of delayed intentions. *Journal of Neuroscience*, *31*(8), 2888–2894. https://doi.org/10.1523/JNEUROSCI.5336-10.2011

Gilbert, S. J., Spengler, S., Simons, J. S., Frith, C. D., & Burgess, P. W. (2005a). Differential functions of lateral and medial rostral prefrontal cortex (area 10) revealed by brain-behavior associations. *Cerebral Cortex*, *16*(12), 1783–1789. https://doi.org/10.1093/cercor/bhj113

Gilbert, S. J., Spengler, S., Simons, J. S., Frith, C. D., & Burgess, P. W. (2005b). Differential Functions of Lateral and Medial Rostral Prefrontal Cortex (Area 10) Revealed by Brain-Behavior Associations. *Cerebral Cortex*, *16*(12), 1783–1789. https://doi.org/10.1093/cercor/bhj113

Gluth, S., Sommer, T., Rieskamp, J., & Büchel, C. (2015). Effective connectivity between hippocampus and ventromedial prefrontal cortex controls preferential choices from memory. *Neuron*, *86*(4), 1078–1090. https://doi.org/10.1016/j.neuron.2015.04.023

Gorgolewski, K. (2016). Nipype: A flexible, lightweight and extensible neuroimaging data processing framework in Python. *Frontiers in Neuroinformatics*, 15.

Graybiel, A. M. (1995). Building action repertoires: Memory and learning functions of the basal ganglia. *Current Opinion in Neurobiology*, *5*(6), 733–741. https://doi.org/10.1016/0959-4388(95)80100-6

Guise, K. G., & Shapiro, M. L. (2017). Medial Prefrontal Cortex Reduces Memory Interference by Modifying Hippocampal Encoding. *Neuron*, *94*(1), 183-192.e8. https://doi.org/10.1016/j.neuron.2017.03.011

Gupta, A. S., van der Meer, M. A., Touretzky, D. S., & Redish, A. D. (2010). Hippocampal replay Is not a simple function of experience. *Neuron*, *65*, 695–705.

Haber, S. N. (2016). Corticostriatal circuitry. *Dialogues in Clinical Neuroscience*, *18*(1), 15.

Haber, S. N., Kim, K.-S., Mailly, P., & Calzavara, R. (2006). Reward-Related Cortical Inputs Define a Large Striatal Region in Primates That Interface with Associative Cortical Connections, Providing a Substrate for Incentive-Based Learning. *Journal of Neuroscience*, *26*(32), 8368–8376. https://doi.org/10.1523/JNEUROSCI.0271-06.2006

Hadj-Bouziane, F., & Boussaoud, D. (2003). Neuronal activity in the monkey striatum during conditional visuomotor learning. *Experimental Brain Research*, *153*(2), 190–196. https://doi.org/10.1007/s00221-003-1592-4

Hadj-Bouziane, F., Frankowska, H., Meunier, M., Coquelin, P.-A., & Boussaoud, D. (2006). Conditional visuo-motor learning and dimension reduction. *Cogn Process*, *7*, 95–104.

Hamm, A. G., & Mattfeld, A. T. (2019). Distinct neural circuits underlie prospective and concurrent memory-guided behavior. *Cell Reports*, *28*(10), 2541–2553. https://doi.org/10.1016/j.celrep.2019.08.002

Han, S., Huettel, S. A., Raposo, A., Adcock, R. A., & Dobbins, I. G. (2010). Functional significance of striatal responses during episodic decisions: Recovery or goal attainment? *Journal of Neuroscience*, *30*(13), 4767–4775.

Hannula, D. E., & Ranganath, C. (2008). Medial Temporal Lobe Activity Predicts Successful Relational Memory Binding. *Journal of Neuroscience*, *28*(1), 116–124. https://doi.org/10.1523/JNEUROSCI.3086-07.2008

Haruno, M., & Kawato, M. (2006). Different neural correlates of reward expectation and reward expectation error in the putamen and caudate nucleus during stimulus-action-reward association learning. *Journal of Neurophysiology*, *95*(2), 948–959. https://doi.org/10.1152/jn.00382.2005

Haynes, J.-D., Sakai, K., Rees, G., Gilbert, S., Frith, C., & Passingham, R. E. (2007). Reading hidden intentions in the human brain. *Current Biology*, *17*, 323–328.

Heidbreder, C. A., & Groenewegen, H. J. (2003). The medial prefrontal cortex in the rat: Evidence for a dorso-ventral distinction based upon functional and anatomical characteristics. *Neuroscience and Biobehavioral Reviews*, *27*, 555–579.

Hindy, N. C., & Turk-Browne, N. B. (2016). Action-Based Learning of Multistate Objects in the Medial Temporal Lobe. *Cerebral Cortex*, *26*(5), 1853–1865. https://doi.org/10.1093/cercor/bhv030

Histed, M. H., Pasupathy, A., & Miller, E. K. (2003). Learning substrates in the primate prefrontal cortex and striatum: Sustained activity related to successful actions. *Neuron*, *63*, 244–253.

Hoover, W. B., & Vertes, R. P. (2007). Anatomical analysis of afferent projections to the medial prefrontal cortex in the rat. *Brain Structure and Function*, *212*(2), 149–179. https://doi.org/10.1007/s00429-007-0150-4

Howard, M. W., & Eichenbaum, H. (2015). Time and space in the hippocampus. *Brain Research*, *1621*, 345–354. https://doi.org/10.1016/j.brainres.2014.10.069

Hsieh, L.-T., Gruber, M. J., Jenkins, L. J., & Ranganath, C. (2014). Hippocampal Activity Patterns Carry Information about Objects in Temporal Context. *Neuron*, *81*(5), 1165–1178. https://doi.org/10.1016/j.neuron.2014.01.015

Jadhav, S. P., Kemere, C., German, P. W., & Frank, L. M. (2012). Awake hippocampal sharp-wave ripples support spatial memory. *Science*, *336*(6087), 1454–1458. https://doi.org/10.1126/science.1217230

Jadhav, S. P., Rothschild, G., Roumis, D. K., & Frank, L. M. (2016). Coordinated excitation and inhibition of prefrontal ensembles during awake hippocampal sharp-wave ripple events. *Neuron*, *90*(1), 113–127. https://doi.org/10.1016/j.neuron.2016.02.010

Jayachandran, M., Linley, S. B., Schlecht, M., Mahler, S. V., Vertes, R. P., & Allen, T. A. (2019). Prefrontal Pathways Provide Top-Down Control of Memory for Sequences of Events. *Cell Reports*, *28*(3), 640-654.e6. https://doi.org/10.1016/j.celrep.2019.06.053

Jenkinson, M., Beckmann, C. F., Behrens, T. E., Woolrich, M. W., & Smith, S. M. (2012). FSL. *NeuroImage*, *62*(2), 782–790. https://doi.org/10.1016/j.neuroimage.2011.09.015

Jiang, J., Brashier, N. M., & Egner, T. (2015). Memory meets control in hippocampal and striatal binding of stimuli, responses, and attentional control states. *Journal of Neuroscience*, *35*(44), 14885–14895.

Johnson, J. D., McDuff, S. G. R., Rugg, M. D., & Norman, K. A. (2009). Recollection, Familiarity, and Cortical Reinstatement: A Multivoxel Pattern Analysis. *Neuron*, *63*(5), 697–708. https://doi.org/10.1016/j.neuron.2009.08.011

Johnson, M., & Johnson, M. (2014). Decoding individual natural scene representations during perception and imagery. *Frontiers in Human Neuroscience*, *8*. https://www.frontiersin.org/article/10.3389/fnhum.2014.00059

Jones, M. W., & Wilson, M. A. (2005a). Phase precession of medial prefrontal cortical activity relative to the hippocampal theta rhythm. *Hippocampus*, *15*(7), 867–873. https://doi.org/10.1002/hipo.20119

Jones, M. W., & Wilson, M. A. (2005b). Theta rhythms coordinate hippocampal–prefrontal interactions in a spatial memory task. *PLoS Biology*, *3*(12), 2187–2199. https://doi.org/10.1371/journal.pbio.0030402

Karlsson, M. P., & Frank, L. M. (2009). Awake replay of remote experiences in the hippocampus. *Nature Neuroscience*, *12*(7), 913–918.

King, D. R., de Chastelaine, M., Elward, R. L., Wang, T. H., & Rugg, M. D. (2015). Recollection-Related Increases in Functional Connectivity Predict Individual Differences in Memory Accuracy. *Journal of Neuroscience*, *35*(4), 1763–1772. https://doi.org/10.1523/JNEUROSCI.3219-14.2015

Kliegel, M., Martin, M., McDaniel, M. A., & Einstein, G. O. (2002). Complex prospective memory and executive control of working memory: A process model. *Psychologische Beitrage*, *44*, 303–318.

Koch, K., Schachtzabel, C., Wagner, G., Reichenbach, J. R., Sauer, H., & Schlösser, R. (2008). The neural correlates of reward-related trial-and-error learning: An fMRI study with a probabilistic learning task. *Learning & Memory*, *15*(10), 728–732. https://doi.org/10.1101/lm.1106408

Köhler, S., Crane, J., & Milner, B. (2002). Differential contributions of the parahippocampal place area and the anterior hippocampus to human memory for scenes. *Hippocampus*, *12*(6), 718–723. https://doi.org/10.1002/hipo.10077

Künzle, H. (1975). Bilateral projections from precentral motor cortex to the putamen and other parts of the basal ganglia. An autoradiographic study in

Macaca fascicularis. *Brain Research*, *88*(2), 195–209. https://doi.org/10.1016/0006-8993(75)90384-4

Kvavilashvili, L. (1987). Remembering intention as a distinct form of memory. *British Journal of Psychology*, *78*(4), 507–518. https://doi.org/10.1111/j.2044-8295.1987.tb02265.x

Law, J. R., Flanery, M. A., Wirth, S., Yanike, M., Smith, A. C., Frank, L. M., Suzuki, W. A., Brown, E. N., & Stark, C. E. (2005). Functional magnetic resonance imaging activity during the gradual acquisition and expression of paired-associate memory. *Journal of Neuroscience*, *25*(24), 5720–5729.

Liljeholm, M., & O'Doherty, J. P. (2012). Contributions of the striatum to learning, motivation, and performance: An associative account. *Trends in Cognitive Sciences*, *16*(9), 467–475. https://doi.org/10.1016/j.tics.2012.07.007

Liu, Z.-X., Shen, K., Olsen, R. K., & Ryan, J. D. (2017). Visual Sampling Predicts Hippocampal Activity. *The Journal of Neuroscience*, *37*(3), 599–609. https://doi.org/10.1523/JNEUROSCI.2610-16.2016

Mahmoudi, A., Takerkart, S., Regragui, F., Boussaoud, D., & Brovelli, A. (2012). Multivoxel pattern analysis for fMRI data: A review. *Computational and Mathematical Methods in Medicine*, *2012*, 1–14. https://doi.org/10.1155/2012/961257

Mai, J. K., Assheuer, J., & Paxinos, G. (2004). *Atlas of the Human Brain*. Elsevier Academic Press.

MathWorks. (2012). *MATLAB and Statistics Toolbox Release* (Version 2012b) [Computer software]. The Math-Works, Inc.

Mattfeld, A. T., & Stark, C. E. (2011). Striatal and medial temporal lobe functional interactions during visuomotor associative learning. *Cerebral Cortex*, *21*(3), 647–658. https://doi.org/10.1093/cercor/bhq144

Mattfeld, A. T., & Stark, C. E. L. (2015). Functional contributions and interactions between the human hippocampus and subregions of the striatum during arbitrary associative learning and memory: ROLES OF THE HIPPOCAMPUS AND STRIATAL SUBREGIONS. *Hippocampus*, *25*(8), 900–911. https://doi.org/10.1002/hipo.22411

McDaniel, M. A., & Einstein, G. O. (2000). Strategic and automatic processes in prospective memory retrieval: A multiprocess framework. *Applied Cognitive Psychology*, *14*(7), S127–S144. https://doi.org/10.1002/acp.775

McDaniel, M. A., LaMontagne, P., Beck, S. M., Scullin, M. K., & Braver, T. S. (2013). Dissociable Neural Routes to Successful Prospective Memory.

Psychological Science, *24*(9), 1791–1800. https://doi.org/10.1177/0956797613481233

McFarland, N. R., & Haber, S. N. (2000). Convergent Inputs from Thalamic Motor Nuclei and Frontal Cortical Areas to the Dorsal Striatum in the Primate. *The Journal of Neuroscience*, *20*(10), 3798–3813. https://doi.org/10.1523/JNEUROSCI.20-10-03798.2000

Miyachi, S., Hikosaka, O., & Lu, X. (2002). Differential activation of monkey striatal neurons in the early and late stages of procedural learning. *Experimental Brain Research*, *146*(1), 122–126. https://doi.org/10.1007/s00221-002-1213-7

Miyachi, S., Hikosaka, O., Miyashita, K., Kárádi, Z., & Rand, M. K. (1997). Differential roles of monkey striatum in learning of sequential hand movement. *Experimental Brain Research*, *115*(1), 1–5. https://doi.org/10.1007/PL00005669

Miyashita, Y., Higuchi, S.-I., Sakai, K., & Masui, N. (1991). Generation of fractal patterns for probing the visual memory. *Neuroscience Research*, *12*, 307–311.

Momennejad, I., & Haynes, J. (2013). Encoding of prospective tasks in the human prefrontal cortex under varying task loads. *Journal of Neuroscience*, *33*(44), 17342–17349. https://doi.org/10.1523/JNEUROSCI.0492-13.2013

Momennejad, I., & Haynes, J.-D. (2012). Human anterior prefrontal cortex encodes the 'what' and 'when' of future intentions. *NeuroImage*, *61*(1), 139–148. https://doi.org/10.1016/j.neuroimage.2012.02.079

Monti, C., Sozzi, M., Corbo, M., Fronda, G., & Balconi, M. (2020). Prospective memories and working memory: Shared resources or distinct mechanisms? *Applied Neuropsychology: Adult*, *27*(4), 311–325. https://doi.org/10.1080/23279095.2018.1550407

Mumford, J. A., Turner, B. O., Ashby, F. G., & Poldrack, R. A. (2012). Deconvolving BOLD activation in event-related designs for multivoxel pattern classification analyses. *NeuroImage*, *59*(3), 2636–2643.

Murty, V. P., Feldman-Hall, O., Hunter, L. E., Phelps, E. A., & Davachi, L. (2016). Episodic memories predict adaptive value-based decision-making. *Journal of Experimental Psychology: General*, *145*(5), 548–558. https://doi.org/10.1037/xge0000158

Norman, Y., Yeagle, E. M., Khuvis, S., Harel, M., Mehta, A. D., & Malach, R. (2019). Hippocampal sharp-wave ripples linked to visual episodic recollection in humans. *Science*, *365*(657), 1–14.

O'Doherty, J., Dayan, P., Schultz, J., Deichmann, R., Friston, K., & Dolan, R. J. (2004). Dissociable roles of ventral and dorsal striatum in instrumental conditioning. *Science*, *304*(5669), 452–454. https://doi.org/10.1126/science.1094285

O'Doherty, J. P., Cockburn, J., & Pauli, W. M. (2017). Learning, reward, and decision making. *Annual Review of Psychology*, *68*(1), 73–100. https://doi.org/10.1146/annurev-psych-010416-044216

Okuda, J., Fujii, T., Ohtake, H., Tsukiura, T., Yamadori, A., Frith, C. D., & Burgess, P. W. (2007). Differential involvement of regions of rostral prefrontal cortex (Brodmann area 10) in time- and event-based prospective memory. *International Journal of Psychophysiology*, *64*(3), 233–246. https://doi.org/10.1016/j.ijpsycho.2006.09.009

Owen, A. M., Doyon, J., Petrides, M., & Evans, A. C. (1996). Planning and Spatial Working Memory: A Positron Emission Tomography Study in Humans. *European Journal of Neuroscience*, *8*(2), 353–364. https://doi.org/10.1111/j.1460-9568.1996.tb01219.x

Palombo, D. J., Keane, M. M., & Verfaellie, M. (2015). How does the hippocampus shape decisions? *Neurobiology of Learning and Memory*, *125*, 93–97. https://doi.org/10.1016/j.nlm.2015.08.005

Park, J., & Park, S. (2015). The representation of texture information in the parahippocampal place area. *Journal of Vision*, *15*(12), 511. https://doi.org/10.1167/15.12.511

Pasupathy, A., & Miller, E. K. (2005). Different time courses of learning-related activity in the prefrontal cortex and striatum. *Nature*, *433*(7028), 873–876. https://doi.org/10.1038/nature03287

Pedregosa, F., Varoquaux, G., Gramfort, A., Michel, V., Thirion, B., Grisel, O., Blondel, M., Prettenhofer, P., Weiss, R., Dubourg, V., Vanderplas, J., Passos, A., & Cournapeau, D. (2011). Scikit-learn: Machine Learning in Python. *MACHINE LEARNING IN PYTHON*, 6.

Peirce, J. W. (2009). Generating stimuli for neuroscience using PsychoPy. *Frontiers in Neuroinformatics*, *2*(10), 1–8. https://doi.org/10.3389/neuro.11.010.2008

Petrides, M. (1997). Visuo-motor conditional associative learning after frontal and temporal lesions in the human brain. *Neuropsychologia*, *35*(7), 989–997. https://doi.org/10.1016/S0028-3932(97)00026-2

Pfeiffer, B. E., & Foster, D. J. (2013). Hippocampal place-cell sequences depict future paths to remembered goals. *Nature*, *497*(7447), 74–79. https://doi.org/10.1038/nature12112

Preston, A. R., & Eichenbaum, H. (2013). Interplay of hippocampus and prefrontal cortex in memory. *Current Biology*, *23*(17), R764–R773. https://doi.org/10.1016/j.cub.2013.05.041

Provost, J.-S., Petrides, M., & Monchi, O. (2010). Dissociating the role of the caudate nucleus and dorsolateral prefrontal cortex in the monitoring of events within human working memory: Functional role of the caudate nucleus. *European Journal of Neuroscience*, *32*(5), 873–880. https://doi.org/10.1111/j.1460-9568.2010.07333.x

Qu, J., Qian, L., Chen, C., Xue, G., Li, H., Xie, P., & Mei, L. (2017). Neural Pattern Similarity in the Left IFG and Fusiform Is Associated with Novel Word Learning. *Frontiers in Human Neuroscience*, *11*, 424. https://doi.org/10.3389/fnhum.2017.00424

Ragozzino, M. E. (2003). Acetylcholine actions in the dorsomedial striatum support the flexible shifting of response patterns. *Neurobiology of Learning and Memory*, *80*(3), 257–267. https://doi.org/10.1016/S1074-7427(03)00077-7

Redish, A. D. (2016). Vicarious trial and error. *Nat Rev Neurosci.*, *17*(3), 147–159.

Reeders, P. C., Hamm, A. G., Allen, T. A., & Mattfeld, A. T. (2021). Medial prefrontal cortex and hippocampal activity differentially contribute to ordinal and temporal context retrieval during sequence memory. *Learning & Memory*, *28*(4), 134–147. https://doi.org/10.1101/lm.052365.120

Remondes, M., & Wilson, M. A. (2013). Cingulate-Hippocampus Coherence and Trajectory Coding in a Sequential Choice Task. *Neuron*, *80*(5), 1277–1289. https://doi.org/10.1016/j.neuron.2013.08.037

Reynolds, J. R., West, R., & Braver, T. (2009). Distinct Neural Circuits Support Transient and Sustained Processes in Prospective Memory and Working Memory. *Cerebral Cortex*, *19*(5), 1208–1221. https://doi.org/10.1093/cercor/bhn164

Rissman, J., Gazzaley, A., & D'Esposito, M. (2004). Measuring functional connectivity during distinct stages of a cognitive task. *NeuroImage*, *23*(2), 752–763. https://doi.org/10.1016/j.neuroimage.2004.06.035

Roche, A. (2011). A Four-Dimensional Registration Algorithm With Application to Joint Correction of Motion and Slice Timing in fMRI. *IEEE Transactions on Medical Imaging*, *30*(8), 1546–1554. https://doi.org/10.1109/TMI.2011.2131152

Schacter, D. L., Benoit, R. G., & Szpunar, K. K. (2017). Episodic future thinking: Mechanisms and functions. *Current Opinion in Behavioral Sciences*, *17*, 41–50. https://doi.org/10.1016/j.cobeha.2017.06.002

Schapiro, A. C., Kustner, L. V., & Turk-Browne, N. B. (2012). Shaping of Object Representations in the Human Medial Temporal Lobe Based on Temporal Regularities. *Current Biology*, *22*(17), 1622–1627. https://doi.org/10.1016/j.cub.2012.06.056

Schapiro, A. C., Rogers, T. T., Cordova, N. I., Turk-Browne, N. B., & Botvinick, M. M. (2013). Neural representations of events arise from temporal community structure. *Nature Neuroscience*, *16*(4), 486–492.

Schapiro, A. C., Turk-Browne, N. B., Norman, K. A., & Botvinick, M. M. (2016). Statistical learning of temporal community structure in the hippocampus. *Hippocampus*, *26*(1), 3–8. https://doi.org/10.1002/hipo.22523

Schedlbauer, A. M., Copara, M. S., Watrous, A. J., & Ekstrom, A. D. (2014). Multiple interacting brain areas underlie successful spatiotemporal memory retrieval in humans. *Scientific Reports*, *4*(1), 6431. https://doi.org/10.1038/srep06431

Schlichting, M. L., & Preston, A. R. (2016). Hippocampal–medial prefrontal circuit supports memory updating during learning and post-encoding rest. *Neurobiology of Learning and Memory*, *134*, 91–106. https://doi.org/10.1016/j.nlm.2015.11.005

Schultz, W., Tremblay, L., & Hollerman, J. R. (2003). Changes in behavior-related neuronal activity in the striatum during learning. *Trends in Neurosciences*, *26*(6), 321–328. https://doi.org/10.1016/S0166-2236(03)00122-X

Scullin, M. K., McDaniel, M. A., Shelton, J. T., & Lee, J. H. (2010). Focal/nonfocal cue effects in prospective memory: Monitoring difficulty or different retrieval processes? *Journal of Experimental Psychology: Learning, Memory, and Cognition*, *36*(3), 736–749. https://doi.org/10.1037/a0018971

Selemon', L. D., & Goldman-Rakic, P. S. (1985). Longitudinal Topography and Interdigitation of Corticostriatal Projections in the Rhesus Monkey'. *The Journal of Neuroscience*, *5*(3), 19.

Shin, J. D., & Jadhav, S. P. (2016). Multiple modes of hippocampal–prefrontal interactions in memory-guided behavior. *Current Opinion in Neurobiology*, *40*, 161–169. https://doi.org/10.1016/j.conb.2016.07.015

Shin, J. D., Tang, W., & Jadhav, S. P. (2019). Dynamics of awake hippocampal-prefrontal replay for spatial learning and memory-guided decision making. *Neuron*, *104*(6), 1110–1125. https://doi.org/10.1016/j.neuron.2019.09.012

Shohamy, D., & Daw, N. D. (2015). Integrating memories to guide decisions. *Current Opinion in Behavioral Sciences*, *5*, 85–90. https://doi.org/10.1016/j.cobeha.2015.08.010

Simons, J. S., Scholvinck, M. L., Gilbert, S. J., Frith, C. D., & Burgess, P. W. (2006). Differential components of prospective memory? Evidence from fMRI. *Neuropsychologia*, *44*(8), 1388–1397. https://doi.org/10.1016/j.neuropsychologia.2006.01.005

Singer, A. C., Carr, M. F., Karlsson, M. P., & Frank, L. M. (2013). Hippocampal SWR Activity Predicts Correct Decisions during the Initial Learning of an Alternation Task. *Neuron*, *77*(6), 1163–1173. https://doi.org/10.1016/j.neuron.2013.01.027

Skinner, D. M., Martin, G. M., Wright, S. L., Tomlin, J., Odintsova, I. V., Thorpe, C. M., Harley, C. W., & Marrone, D. F. (2014). Hippocampal spatial mapping and the acquisition of competing responses. *Hippocampus*, 396–402.

Smith, A., & Brown, E. (2003). Estimating a state-space model from point process observations. *Neural Computation*, *15*(5), 965–991. https://doi.org/10.1162/089976603765202622

Smith, A. C., Frank, L. M., Wirth, S., Yanike, M., Hu, D., Kubota, Y., Graybiel, A. M., Suzuki, W. A., & Brown, E. N. (2004). Dynamic analysis of learning in behavioral experiments. *Journal of Neuroscience*, *24*(2), 447–461. https://doi.org/10.1523/JNEUROSCI.2908-03.2004

Smith, S. M., & Brady, J. M. (1997). *SUSAN—A New Approach to Low Level Image Processing*. 34.

Soon, C. S., Brass, M., Heinze, H.-J., & Haynes, J.-D. (2008). Unconscious determinants of free decisions in the human brain. *Nature Neuroscience*, *11*(5), 543–545. https://doi.org/10.1038/nn.2112

Squire, L. R. (1992). Memory and the hippocampus: A synthesis from findings with rats, monkeys, and humans. *Psychological Review*, *99*(2), 195–231.

Squire, L. R., Stark, C. E., & Clark, R. E. (2004). The medial temporal lobe. *Annual Review of Neuroscience*, *27*(1), 279–306. https://doi.org/10.1146/annurev.neuro.27.070203.144130

Stark, S. M., Frithsen, A., Mattfeld, A. T., & Stark, C. E. (2018). Modulation of associative learning in the hippocampal-striatal circuit based on item-set similarity. *Cortex*, *109*, 60–73.

Sun, L., Frank, S. M., Epstein, R. A., & Tse, P. U. (2021). The parahippocampal place area and hippocampus encode the spatial significance of landmark objects. *NeuroImage*, *236*, 118081. https://doi.org/10.1016/j.neuroimage.2021.118081

Tang, W., Shin, J. D., Frank, L. M., & Jadhav, S. P. (2017). Hippocampal-prefrontal reactivation during learning is stronger in awake compared with sleep states. *Journal of Neuroscience*, *37*(49), 11789–11805. https://doi.org/10.1523/JNEUROSCI.2291-17.2017

Tremblay, L., Hollerman, J. R., & Schultz, W. (1998). Modifications of reward expectation-related neuronal activity during learning in primate striatum. *Journal of Neurophysiology*, *80*(2), 964–977. https://doi.org/10.1152/jn.1998.80.2.964

Tricomi, E. M., Delgado, M. R., & Fiez, J. A. (2004). Modulation of caudate activity by action contingency. *Neuron*, *41*(2), 281–292. https://doi.org/10.1016/S0896-6273(03)00848-1

Tse, D., Langston, R. F., Kakeyama, M., Bethus, I., Spooner, P. A., Wood, E. R., Witter, M. P., & Morris, R. G. (2007). Schemas and memory consolidation. *Science*, *316*(5821), 76–82. https://doi.org/10.1126/science.1135935

van den Hurk, J., Gentile, F., & Jansma, B. (2011). What's behind a face: Person context coding in fusiform face area as revealed by multivoxel pattern analysis. *Cerebral Cortex*, *21*(12), 2893–2899. https://doi.org/10.1093/cercor/bhr093

van der Meer, M., Kurth-Nelson, Z., & Redish, A. D. (2012). Information Processing in Decision-Making Systems. *The Neuroscientist*, *18*(4), 342–359. https://doi.org/10.1177/1073858411435128

van Kesteren, M. T. R., Brown, T. I., & Wagner, A. D. (2018). Learned Spatial Schemas and Prospective Hippocampal Activity Support Navigation After One-Shot Learning. *Frontiers in Human Neuroscience*, *12*, 486. https://doi.org/10.3389/fnhum.2018.00486

van Kesteren, M. T., Rijpkema, M., Ruiter, D. J., & Fernandez, G. (2010). Retrieval of associative information congruent with prior knowledge is related to increased medial prefrontal activity and connectivity. *Journal of Neuroscience*, *30*(47), 15888–15894. https://doi.org/10.1523/JNEUROSCI.2674-10.2010

Vertes, R. P. (2006). Interactions among the medial prefrontal cortex, hippocampus and midline thalamus in emotional and cognitive processing in the rat. *Neuroscience*, *142*(1), 1–20. https://doi.org/10.1016/j.neuroscience.2006.06.027

Volle, E., Gonen-Yaacovi, G., de Lacy Costello, A., Gilbert, S. J., & Burgess, P. W. (2011). The role of rostral prefrontal cortex in prospective memory: A voxel-based lesion study. *Neuropsychologia*, *49*(8), 2185–2198. https://doi.org/10.1016/j.neuropsychologia.2011.02.045

Wang, S.-H., & Morris, R. G. (2010). Hippocampal-neocortical interactions in memory formation, consolidation, and reconsolidation. *Annual Review of Psychology*, *61*(1), 49–79. https://doi.org/10.1146/annurev.psych.093008.100523

Weaverdyck, M. E., Lieberman, M. D., & Parkinson, C. (2020). Multivoxel pattern analysis in fMRI: A practical introduction for social and affective neuroscientists. *Social Cognitive and Affective Neuroscience*, *15*(4), 487–509. https://doi.org/10.1093/scan/nsaa057

Weber, E. U., Bockenholt, U., Hilton, D. J., & Wallace, B. (1993). Determinants of diagnostic hypothesis generation: Effects of information, base rates, and experience. *Journal of Experimental Psychology: Learning, Memory, and Cognition*, *19*(5), 1151–1164.

Wimmer, G. E., & Shohamy, D. (2012). Preference by association: How memory mechanisms in the hippocampus bias decisions. *Science*, *338*(6104), 270–273. https://doi.org/10.1126/science.1223252

Wirth, S., Yanike, M., Frank, L. M., Smith, A. C., Brown, E. N., & Suzuki, W. A. (2003). Single neurons in the monkey hippocampus and learning of new associations. *Science*, *300*, 1578–1581.

Xue, G., Dong, Q., Chen, C., Lu, Z., Mumford, J. A., & Poldrack, R. A. (2010). Greater Neural Pattern Similarity Across Repetitions Is Associated with Better Memory. *Science*, *330*(6000), 97–101. https://doi.org/10.1126/science.1193125

Yin, H. H., & Knowlton, B. J. (2004). Contributions of Striatal Subregions to Place and Response Learning. *Learning & Memory*, *11*(4), 459–463. https://doi.org/10.1101/lm.81004

Yin, H. H., Ostlund, S. B., Knowlton, B. J., & Balleine, B. W. (2005). The role of the dorsomedial striatum in instrumental conditioning: Striatum and instrumental conditioning. *European Journal of Neuroscience*, *22*(2), 513–523. https://doi.org/10.1111/j.1460-9568.2005.04218.x

Yu, J. Y., & Frank, L. M. (2015). Hippocampal–cortical interaction in decision making. *Neurobiology of Learning and Memory*, *117*, 34–41. https://doi.org/10.1016/j.nlm.2014.02.002

Zeithamova, D., Dominick, A. L., & Preston, A. R. (2012). Hippocampal and ventral medial prefrontal activation during retrieval-mediated learning supports novel inference. *Neuron*, *75*(1), 168–179. https://doi.org/10.1016/j.neuron.2012.05.010

Zeithamova, D., Gelman, B. D., Frank, L., & Preston, A. R. (2018). Abstract Representation of Prospective Reward in the Hippocampus. *The Journal of Neuroscience*, *38*(47), 10093–10101. https://doi.org/10.1523/JNEUROSCI.0719-18.2018

Zeithamova, D., & Preston, A. R. (2010). Flexible memories: Differential roles for medial temporal lobe and prefrontal cortex in cross-episode binding. *Journal of Neuroscience*, *30*(44), 14676–14684. https://doi.org/10.1523/JNEUROSCI.3250-10.2010

Zeithamova, D., Schlichting, M. L., & Preston, A. R. (2012). The hippocampus and inferential reasoning: Building memories to navigate future decisions. *Frontiers in Human Neuroscience*, *6*. https://doi.org/10.3389/fnhum.2012.00070

Zhang, J., Liu, J., & Xu, Y. (2015). Neural Decoding Reveals Impaired Face Configural Processing in the Right Fusiform Face Area of Individuals with Developmental Prosopagnosia. *Journal of Neuroscience*, *35*(4), 1539–1548. https://doi.org/10.1523/JNEUROSCI.2646-14.2015

Appendix 1: Supplemental Material for Chapter 2

Table S1. Voxel mask sizes and peak coordinates for whole-brain contrasts. Related to Figures 2, 3, and 6.

	Voxels	
ROI Mask	Mean	STD
Hippocampus (HPC)	483.40	50.39
Anterior Cingulate Cortex (ACC)	502.65	64.23
Dorsal Anterior Caudate	279.70	30.57
Putamen	650.35	82.93
Dorsolateral Prefrontal Cortex (dlPFC)	459.94	50.53
Motor Cortex	1911.56	203.54

Fixed Before Correct Conditional > Fixed Before Incorrect Conditional

	Peak Voxel (MNI152)			
Cluster Index	**X**	**Y**	**Z**	**Cluster Size**
1	-62	-10	2	544981
2	-55	27	1	588
3	56	27	-4	280
4	-6	-51	-56	176
5	41	35	2	116

Conditional Correct > Fixed Correct

	Peak Voxel (MNI152)			
Cluster Index	**X**	**Y**	**Z**	**Cluster Size**
1	43	-38	46	76219
2	33	19	3	29185
3	-34	17	0	23599
4	-11	5	-3	11888
5	4	25	45	8475
6	10	6	-1	3577
7	4	-75	-19	1817
8	-27	-80	-49	574
9	14	8	71	225
10	35	-70	-49	166

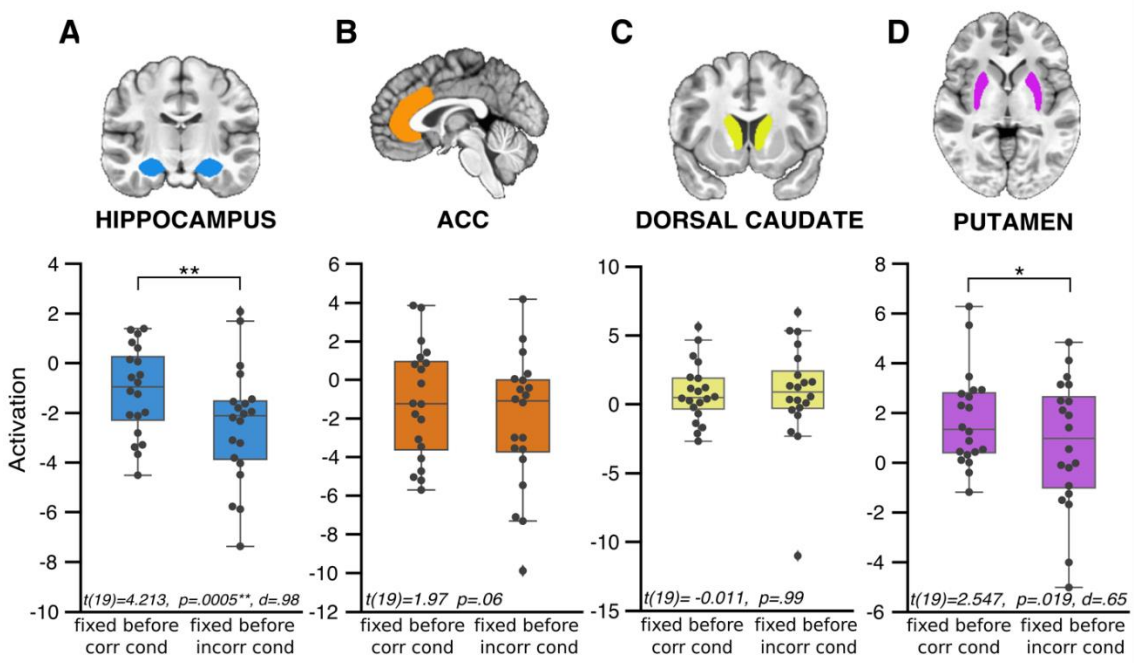

Figure S1. Fixed trial activations preceding correct and incorrect conditional trials for only correct fixed trials. Related to Figure 2. Anatomical regions of interest included the: (A) hippocampus, (B) anterior cingulate cortex (ACC), (C) dorsal caudate, and (D) putamen. Boxplots with overlaid swarm plots represent the activations for only correct fixed trials preceding correct (corr cond) and incorrect (incorr cond) conditional trials. Similar to the original analysis, significantly greater activation was observed in the (A) hippocampus and (D) putamen during correct fixed trials that preceded correct compared to incorrect conditional trials.

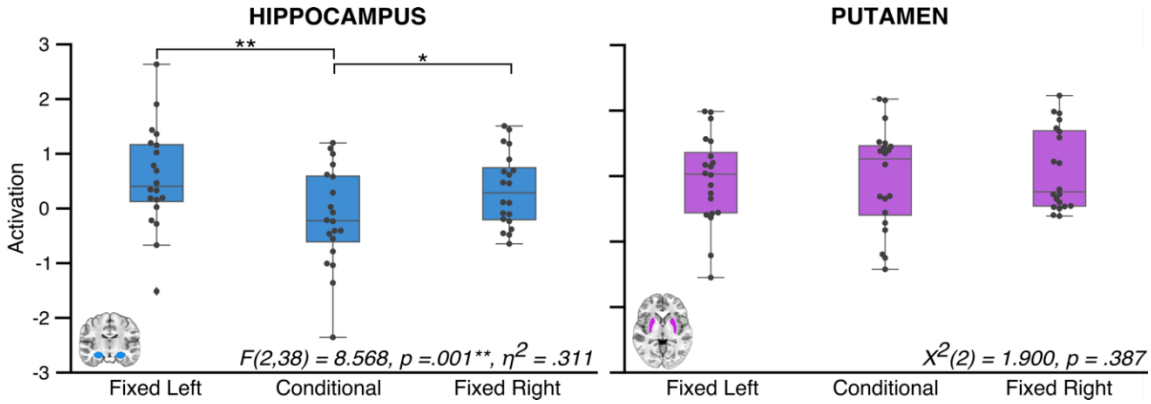

Figure S2. Activations for correct-only fixed-left, conditional, and fixed-right trials in HPC and PUT. Related to Figure 2. Boxplots with overlaid swarm plots represent the activations for the correct learning trial types. In the hippocampus (blue, left) learning trials were significantly different from each other. Fixed-left (.517 ± .21) and fixed-right (.299 ± .15) were significantly greater than conditional (-.201 ± .20) trials (p's < .019). No significant difference was found between fixed-left and fixed-right trials (t(19) = 1.27, p = .221). No significant differences were observed for trial type in the putamen (purple, right). *p < .05; **p < .001.

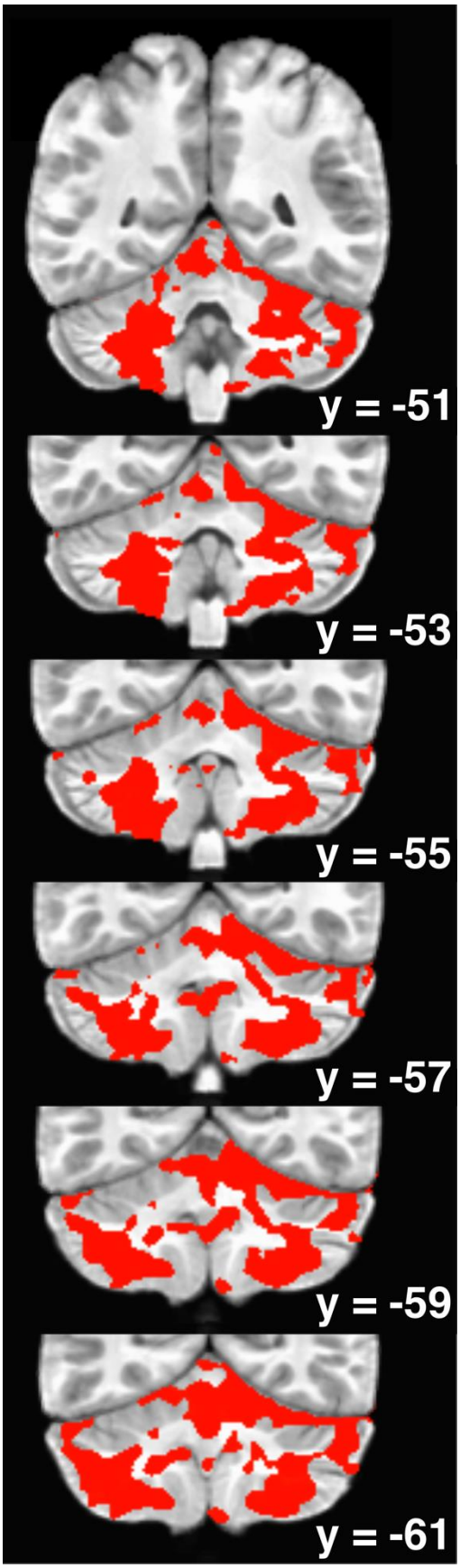

Figure S3. Prospective cerebellar activations for successful memory-guided conditional behavior. Related to Figure 3. Regions of the cerebellum exhibiting greater activation for fixed trials before correct conditional trials > fixed trials before incorrect conditional trials following whole-brain exploratory analysis (FWE tfce corrected $p < 0.05$).

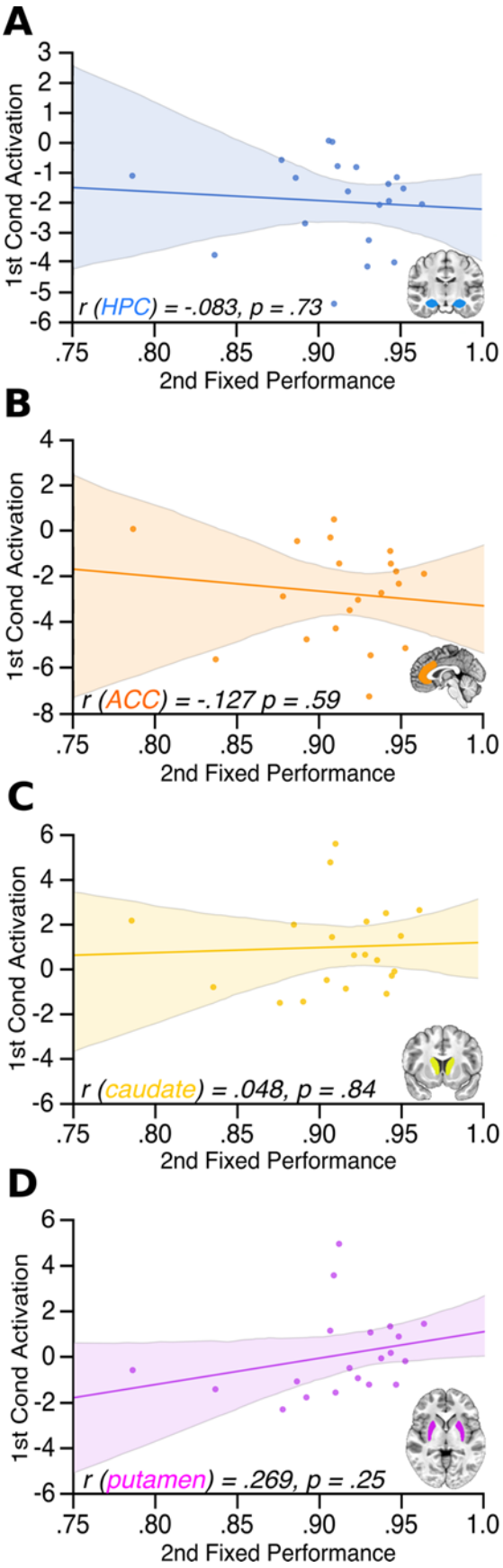

Figure S4. Prospective conditional trial activation correlations with subsequent fixed trial performance. Related to Figure 4. Correlations between preceding conditional trial activation and subsequent fixed trial performance trial pairs. No significant correlation between prior conditional activation and subsequent fixed performance was found for the (A) hippocampus, (B) anterior cingulate cortex, (C) dorsal caudate, or (D) putamen.

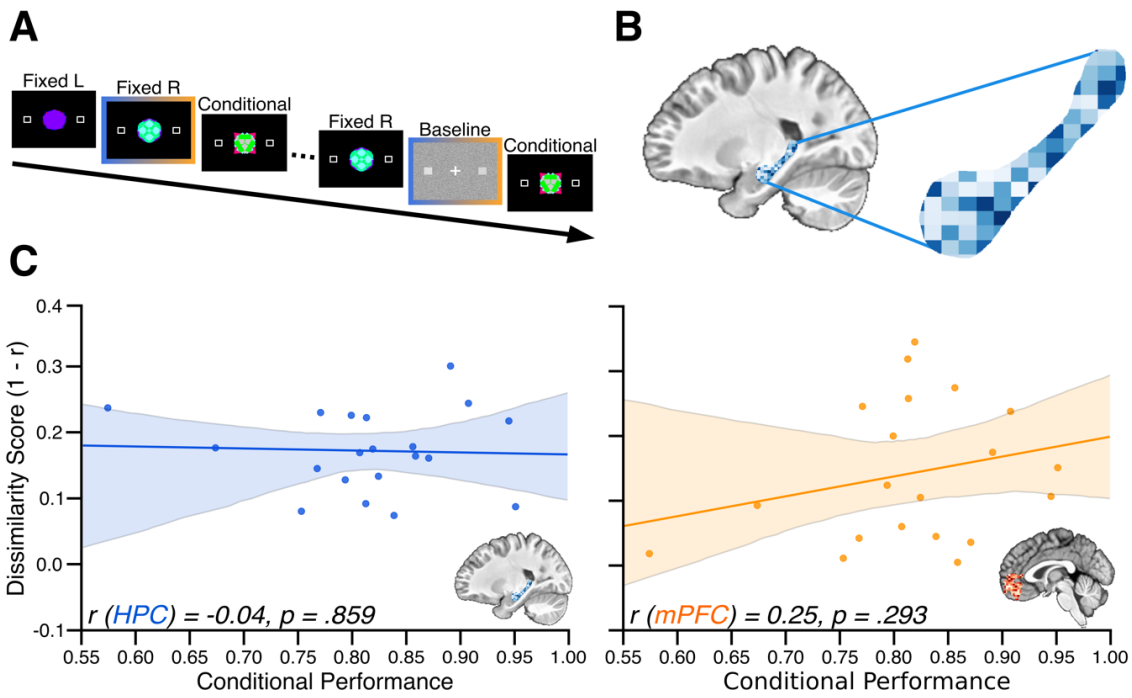

Figure S5. Representational similarity analysis comparing fixed trials that proceed correct conditionals to single baseline trials that intercede between fixed and conditional trials. Related to Figure 2. (A) I compared patterns of activation across voxels in the bilateral hippocampus (B) and voxels in the medial prefrontal cortex that were responsive to the task for fixed trials that proceeded correct conditionals and baseline trials that fell between fixed and conditional trials. (C) A dissimilarity score of 1-r was calculated and correlated with performance on the conditional trials that followed baseline trials. No significant relationship between representational dissimilarity and conditional performance was identified.

Appendix 2: Supplemental Material for Chapter 4

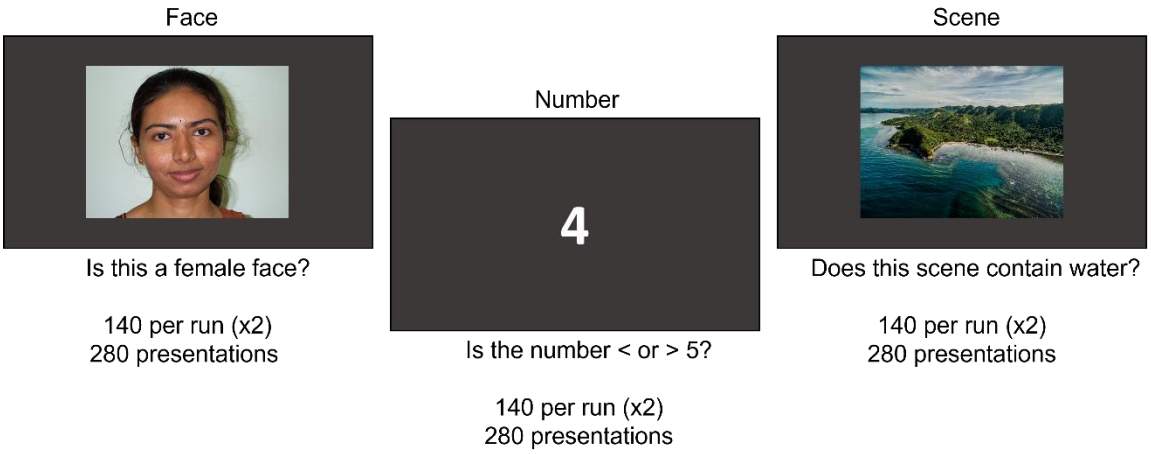

Figure S6. Examples of stimulus categories for functional localizer task. During the functional localizer task, participants were presented with three distinct trial blocks. (*Face*) A male or female face is presented and the participant is asked to indicate whether the face is female. (*Scene*) Participants must indicate if presented scene images contain a body of water. (*Number*) Participants determine if presented numbers are less than or greater than five. Blocks were ordered in face-number-scene-number format, repeated seven times, for a total of 140 presentations of each stimulus per run. For face and scene trials, a left response indicated “Yes” and right indicated “No”. For number trials, left indicated “less than”, while right indicated “greater than”.

VITA

AMANDA G RENFRO-HAMM

2000 - 2006	B.A., Paralegal Science Eastern Kentucky University Richmond, Kentucky
2011-2013	B.S., Psychology Eastern Kentucky University Richmond, Kentucky
2013 - 2015	M.S., Experimental Psychology Eastern Kentucky University Richmond, Kentucky
2015 - 2018	M.S., Psychology, Cognitive Neuroscience Florida International University Miami, Florida
2015 - 2022	Doctoral Candidate Florida International University Miami, Florida

PUBLICATIONS & PRESENTATIONS

Hamm, A.G. & Mattfeld, A.T. (2019). Distinct neural circuits underlie prospective and concurrent memory-guided behavior. *Cell Reports, 28,* 2541-2553.

Renfro, A.G., Antoine, K., & Lawson, A.L. (2013). Sensation seeking influences on memory of positive events. *North American Journal of Psychology, 15*(3), 609-622.

Reeders, P.C., Hamm, A.G., Allen, T.A., & Mattfeld, A.T. (2021). Medial prefrontal cortex and hippocampal activity differentially contribute to ordinal and temporal context retrieval during sequence memory. *Learning & Memory, 28,* 134-147.

Varakin, A., Renfro, A., & Hays, J. (2018). Stimulus response compatibility affects duration judgments, not the rate of subjective time. *Psicológica, 39*, 142-163.

Varakin, A., Renfro, A., & Hays, J. (2016). Time perception and stimulus response compatibility. *Journal of Vision, 16,* 1088.

McClellan, D., Varakin, D.A., Renfro, A., & Hays, J. (2018). The magical number 4 limits selection of object categories for encoding into visual long-term memory. *Journal of Vision, 18*, 831.

Wilson, S., Gore, J., Renfro, A., Blake, M., Muncie, E. & Treadway, J. (2016). The tether to home, University connectedness, and the Appalachian student. *Journal of College Student Retention: Research, Theory & Practice, 0*(0), 1-22.

Kimbler, A., Hays, J., Renfro, A., Varakin, A. (2015). Not so moving: Irrelevance blindness with moving irrelevant stimuli. *Journal of Vision, 15,* 440.

April 2020	Renfro, A. *Emerging Differences in Hippocampal and Extrahippocampal Activation Patterns Across Conditional Associative Learning*. Cognitive Neuroscience Colloquium Series, Presentation, Miami, FL
November 2019	Renfro, A. & Mattfeld, A.T. *Learning-Related Changes in Hippocampal and Caudate Activations in Conditional Associations*. Society for Neuroscience 49th Annual Meeting, Poster Presentation, Chicago, IL
May 2018	Renfro, A. *Differential Functional Interactions Between HPC-mPFC and Caudate-dlPFC During Conditional Associative Learning*. Florida Consortium on the Neurobiology of Cognition, Symposium, Gainesville, FL
January 2018	Renfro, A. & Mattfeld, A.T. *Learning-Related Changes in Hippocampal and Caudate Activations in Conditional Associations*. Park City Winter Conference on the Neurobiology of Learning and Memory, Presentation, Park City, UT
November 2017	Renfro, A. & Mattfeld, A.T. *Beyond Spatial Mapping*: *Unique Mechanisms of Visuomotor Associative Learning.* Society for Neuroscience 47th Annual Meeting, Poster Presentation, Washington DC
May 2017	Renfro, A. & Mattfeld, A.T*. More than Space: Hippocampal Contributions to Associative Learning*. Florida Consortium on the Neurobiology of Cognition, Symposium, Gainesville, FL
February 2017	Renfro, A. & Salo, T. *Open Science Tools for Cognitive Neuroscience.* BrainHack, Symposium, Miami, FL